Special Session, "A tribute to Edilton Santos, a leader in Precambrian Geology in Northeastern Brazil", edited by A.N. Sial and V.P. Ferreira

DOI: 10.1590/2317-4889202020190127

BJGEO Brazilian Journal of Geology

Petrogenesis of the Riacho do Icó Stock: evidence for Neoproterozoic slab melting during accretion tectonics in the Borborema Province?

Lauro Cézar Montefalco de Lira Santos[1]*, Haroldo Monteiro Lima[2], Geysson de Almeida Lages[3], Fabrício de Andrade Caxito[4], José Ferreira de Araújo Neto[1], Ignez de Pinho Guimarães[1,2]

Abstract

One of the main characteristics of the Borborema Province in northeastern Brazil is the abundance of granitic domains. The Lagoa das Pedras plutonic-volcanic Complex record remnants of early to late Neoproterozoic primitive to highly evolved magmas. U-Pb SHRIMP determinations and whole-rock geochemistry on the granitic to granodioritic Riacho do Icó Stock, which is the largest plutonic body of this complex, were conducted. Zircon dating reveals that this body was intruded in the crust at 607 ± 3 Ma, whereas metamorphic overgrowths are coeval within uncertainty (600 ± 8 Ma). Geochemical characteristics of this stock suggest that it corresponds to Cordilleran-type magmas injected in the lithosphere above a subduction zone. Sr and Y contents in addition to MgO and SiO_2 values are compatible with high-silica adakite-like magmas, interpreted as the result of slab melting in deep-seated regions. Based on the integration of this study and literature data, we suggest that the Riacho do Icó intrusion might be a dismembered part of a major continental magmatic arc described in the Central Subprovince of the Borborema Province, marking the onset of the accretionary stage of the Brasiliano orogeny.

KEYWORDS: Arc-related to syn-collisional magmatism; possible slab melting episode; accretion tectonics.

INTRODUCTION

The generation and emplacement of granitic magmas in the lithosphere has always been a thought-provoking topic for the geological community, once that the proposed petrogenetic processes are quite variable for distinct geological periods and environments (*e.g.* Chappell & White 1974, Barbarin 1999, Martin *et al.* 2005, Bonin 2007, Rollinson 2009). Indeed, the investigation of the origin of granitic rocks is critical to understand the evolution of the continental crust, as they represent key records of its growth, recycling, and preservation (Dhuime *et al.* 2012, Hawkesworth *et al.* 2010).

Magma emplacement in the crust is most likely associated to space creation in highly deformed regions, which is triggered by the crustal flow (Paterson & Fowler Jr. 1993). In spite of the variety of the proposed mechanisms for plutonic emplacement — including diapirism, ballooning, and stopping —, their practical application may be confusing (see Petford *et al.* 2000 for details), resulting in a number of geochemical and geophysical modeling proposals (*e.g.* Kusumoto & Takemura 2003, Magee *et al.* 2016, Rochira *et al.* 2018). Nevertheless, there is a longstanding consensus that granitic magmas can be generated in a wide range of geological settings, and are valuable markers to investigate crustal and mantle sources. For instance, peraluminous magmas are generally interpreted as the result of partial melting of metasedimentary rocks in collisional zones (Chappell & White 2001), calc-alkaline rocks are typically found in volcanic arcs above subduction zones (Sheth *et al.* 2002) and plagiogranites are interpreted as final products of partial melting and fractionation of basaltic sources in intra-oceanic settings (Koepke *et al.* 2006).

One of the main features of the Borborema Province in northeastern Brazil is the vast number of granitic batholiths and stocks that are closely related to the regional deformation imposed by the Brasiliano-Pan African Orogeny (650–500 Ma; Santos & Medeiros 1999, Brito Neves *et al.* 2000, 2014). Among them, one of the most intriguing composite plutonic-volcanic domains of the central Borborema Province is the Lagoa das Pedras Complex, which represents a unique record of long-lived superimposed magmatic pulses that were later affected by regional deformation and metamorphism (960–600 Ma; Santos 1995). It is composed of a sequence of mafic-ultramafic rocks interpreted as ophiolite remnants and arc root-related magmas aged at c. 1.0 Ga (Serrote das Pedras Pretas Suite), coeval metagranites and anatexites (Recanto and Riacho do Forno suites), as well as relics of late Neoproterozoic plutons (Riacho do Icó, São João and Serra do Arapuá; Santos 1995, Kozuch 2003).

[1]Universidade Federal de Pernambuco – Recife (PE), Brazil. E-mails: lauromontefalco@gmail.com, araujoneto.geo@gmail.com, ignez@ufpe.br

[2]Universidade Federal do Ceará – Fortaleza (CE), Brazil. E-mail: harolgogeologo@gmail.com

[3]Serviço Geológico do Brasil – Recife (PE), Brazil. E-mail: geysson.lages@cprm.gov.br

[4]Universidade Federal de Minas Gerais – Belo Horizonte (MG), Brazil. E-mail: facaxito@yahoo.com.br

*Corresponding author.

Within this complex, the Riacho do Icó stock represents the largest plutonic pulse, presenting both magmatic structures (enclaves, magmatic foliation, and xenoliths) and tectonic markers (ductile and brittle-related). In this paper, the main geological and geochemical characteristics of the Riacho do Icó stock are explored and their first U-Pb zircon determinations are presented in order to contribute to the understanding of the Neoproterozoic crustal evolution of the Borborema Province.

GEOLOGICAL SETTING

Borborema Province

The Borborema Province (Almeida *et al.* 1981) is characterized by minor Archean blocks that are surrounded by Paleoproterozoic basement domains/terranes, as well as major Meso- to Neoproterozoic supracrustal sequences (Brito Neves *et al.* 2000, Van Schmus *et al.* 1995, 2003, Dantas *et al.* 2013, Ganade de Araújo *et al.* 2014a, Fetter *et al.* 2003, Santos *et al.* 2015, Costa *et al.* 2018). In West Gondwana reconstructions, its continuation can be traced into West Africa through Benin, Nigeria, and Cameroon (Fig. 1; Brito Neves 1975, Trompette 1994, Van Schmus *et al.* 2008, Ganade de Araújo *et al.* 2016), being commonly divided into northern, central/Transversal and southern subprovinces (Van Schmus *et al.* 1995, Santos & Medeiros 1999, Brito Neves *et al.* 2000).

Granitic domains are abundant and precisely record distinct stages of the Brasiliano orogeny (pre-, syn- and post-tectonic magmatism), having been intensively investigated for decades (Almeida *et al.* 1967, Sial 1987, Santos & Medeiros

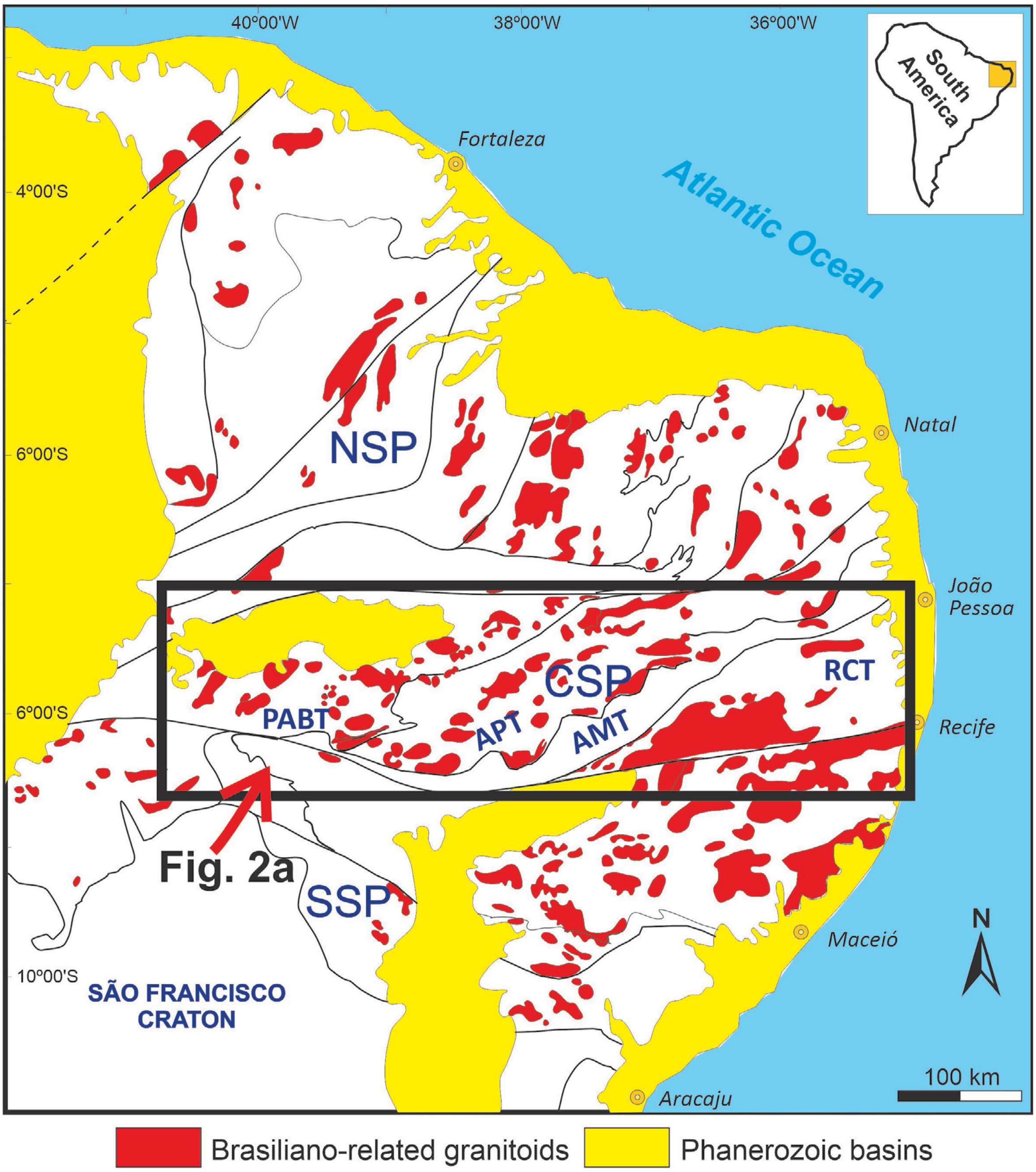

NSP: northern subprovince; CSP: central subprovince; SSP: southern subprovince; PABT: Piancó Alto Brigida Terrane; APT: Alto Pajeú Terrane; AMT: Alto Moxotó Terrane; RCT: Rio Capibaribe Terrane.

Figure 1. Tectonic framework of the Borborema Province with the Brasiliano-related granites highlighted, modified from Brito Neves et al. (2000).

1999, Guimarães & Silva Filho 2000, Guimarães *et al.* 2005, Ferreira *et al.* 2003, Neves *et al.* 2006, Brito Neves *et al.* 2016). A review of the overall petrological aspects of the granites can be found in Ferreira *et al.* (1998), Van Schmus *et al.* (2011), and Sial & Ferreira (2016).

The crustal architecture of the northern subprovince records a series of rocks with magmatic arc affinity ranging from Archean to Neoproterozoic in age, as well as the best-preserved high to ultra-high pressure metamorphic assemblages of the Borborema Province (Nascimento *et al.* 2015, Ganade de Araújo *et al.* 2014b, Santos *et al.* 2014). The Central Subprovince is interpreted as the result of a complex crustal assembly history during the Neoproterozoic, limited by expressive NE-SW shear zones. It comprises the São José do Caiano, Piancó-Alto Brígida, Alto Pajeú, Alto Moxotó, and Rio Capibaribe domains/terranes. Terrane assembly and plate tectonics processes such as subduction and continental collision have been invoked as responsible for the Neoproterozoic crustal building of this area (*e.g.*, Santos & Medeiros 1999, Kozuch 2003, Medeiros 2004, Santos *et al.* 2010, 2014, 2017b, Brito Neves *et al.* 2016, Basto *et al.* 2019), but intracontinental orogenesis is also regarded (Neves 2015).

The southern subprovince includes the marginal fold belts that have tectonic vergence toward the São Francisco Craton in the south: *i.e.* Sergipano, Riacho do Pontal, and Rio Preto belts, as well as the Pernambuco-Alagoas Domain. Archean to early Neoproterozoic rocks are present; however, remnants of Ediacaran subduction-related rocks are interpreted as the main crust forming markers of this subprovince evolution (Silva Filho *et al.* 2010, Oliveira *et al.* 2010, Lima *et al.* 2018, 2019, Caxito *et al.* 2014a, 2016, Alcântara *et al.* 2017); important oceanic crust remnants of probable Cryogenian age fingerprint Neoproterozoic plate tectonics processes in this region (Caxito *et al.* 2014b).

The Alto Pajeú Terrane and the Lagoa das Pedras Complex

The Alto Pajeú Terrane is bounded to the Alto Moxotó and Piancó Alto Brígida terranes by the Serra de Jabitacá Nappe and Riacho do Caboclo Shear Zone, respectively (Santos & Medeiros 1999, Santos *et al.* 2017b, 2018). Unlike other domains of the Borborema Province, Paleoproterozoic crust is rare and the general lithostratigraphic record comprises metaplutonic and supracrustal rocks related to the Stenian-Tonian Cariris Velhos Event (1.0–0.9 Ga; Santos *et al.* 2010). The general geochemical and isotope signature of metagranites, orthogneisses and metavolcanic sequences points out to an episode of ocean-continent convergence (Kozuch 2003, Santos *et al.* 2010, Caxito *et al.* 2014a), including preserved ophiolite remnants (Lages & Dantas 2016). However, based on the geochemistry of Cariris Velhos metaplutonic units, Guimarães *et al.* (2016) suggest instead that these rocks correspond to magmas generated in a within-plate regime. Calc-alkaline and shoshonitic granitoids intrude these sequences, ranging from 650 to 620 Ma (Sial & Ferreira 2016 and references therein).

The São Caetano Complex corresponds to the largest unit of the Alo Pajeú Terrane, hosting most of the granitic intrusions. This complex encompasses metasedimentary and metavolcanic rocks, aged 806 (Guimarães *et al.* 2012) and 858 Ma (Santos *et al.* 2019), being in contact with the Lagoa das Pedras Complex (Fig. 2), which corresponds to a set of (meta)plutonic/volcanic rocks deformed by NE-SW shear zones that impose regional folding (Lima *et al.* 1985). Such structural arrangement is related to the thrust structure that bounds these rocks against the Archean and Paleoproterozoic crust of the Alto Moxotó Terrane (Santos *et al.* 2017a, Lages *et al.* 2019) and the strong influence of a regional sinistral strike-slip splay of shear zones known as Afogados da Ingazeira Shear System (Santos 1995).

The Lagoa das Pedras Pretas Complex occupies an area of 800 km^2, being divided into two geochronological groups:

- Stenian-Tonian;
- Ediacaran intrusions.

The oldest unit is the 1.0 Ga Serrote das Pedras Pretas mafic-ultramafic suite. It is composed of metagabbros, amphibolites, peridotites, and metapyroxenites that form a cluster of gently folded small bodies and lenses characterized by eclogitic mineral assemblages as well as Fe-Ti-V mineralization (Santos 1995, Lages & Dantas 2016).

Granites with ages ranging from 960 to 920 Ma include the Recanto and Riacho do Forno plutons that are interpreted as the result of regional anatexis, cropping out as tabular sheets along SSE-verging thrust surfaces. The former occurs as metagranodiorites to metamonzogranites, and might bear *augen* and mylonitic structures, whereas the latter is characterized by local migmatization, showing well-developed neosome and strongly folded leucosome layers, including two mica diatexites. Lastly, the Riacho do Icó Stock is the dominant late Neoproterozoic granitic body, being coeval to similar granitic intrusions, such as the Serra do Arapuá, São Pedro and São João granites.

THE RIACHO DO ICÓ STOCK

Field relationships

The Riacho do Icó stock displays *en cornue* shape oriented in the E-W direction; its tail follows the NE trend of the Afogados da Ingazeira Shear Zone as the result of crustal shortening and shearing. In the mesoscopic scale, rocks from this intrusion are mostly leucocratic and can be divided into two well-defined facies. In the core of the intrusion, coarse-grained to porphyritic biotite- and amphibole-bearing granites predominate. The magmatic fabric is characterized by the orientation of amphibole clots and potassic feldspar phenocrystals that delineate a moderately developed magmatic foliation. The central portion of the intrusion presents, 2 to 12 cm-ranged subrounded to elliptic mafic (dioritic) autholiths (Fig. 3A), whereas amphibolitic, gneissic, breccia-type, and mylonitic xenoliths (Fig. 3B) are widespread and interpreted as relicts of early Neoproterozoic host-rocks units such as the São Caetano Complex.

Mega xenoliths/roof pendants of ultramafic rocks including Ti-bearing ore bodies of the Serrote das Pedras Pretas Suite

(SPP) cover large areas in the interior of the stock (Fig. 3C). This region is also characterized by local nappes, including tabular granitic sheets that partially obliterate early magmatic fabrics, being interpreted as the first tectonic overprint within the stock. Deformed members of this facies show low-dipping foliations and inclined mica-bearing planes with crenulated lineations that gently dip toward the inner portions of the stock (Fig. 3D).

The second facies on the Riacho do Icó Stock occurs on its southern margin. Progressive deformation related to the Afogados da Ingazeira Shear Zone imposes strain gradation from tabular granitic sheets to gneissic and mylonitic members. Strongly deformed members (*e.g.*, the NE tail) include planar-linear tectonites with sub- to vertical foliation planes (> 65º) that are associated with biotite, amphibole, and muscovite-rich horizontal mineral stretching lineations. Such markers associated with mesoscale kinematic criteria, including S-C type surfaces and σ-type porphyroclasts (Fig. 3E) confirm the sinistral vorticity of the related ductile structures, whereas C' extensional shear bands and asymmetric boudins indicate a transition between strike-slip and extensional regimes. Along the granitic boundaries, the contact between the intrusion and host rocks is tectonic, but chilled margins can be observed (Fig. 3F).

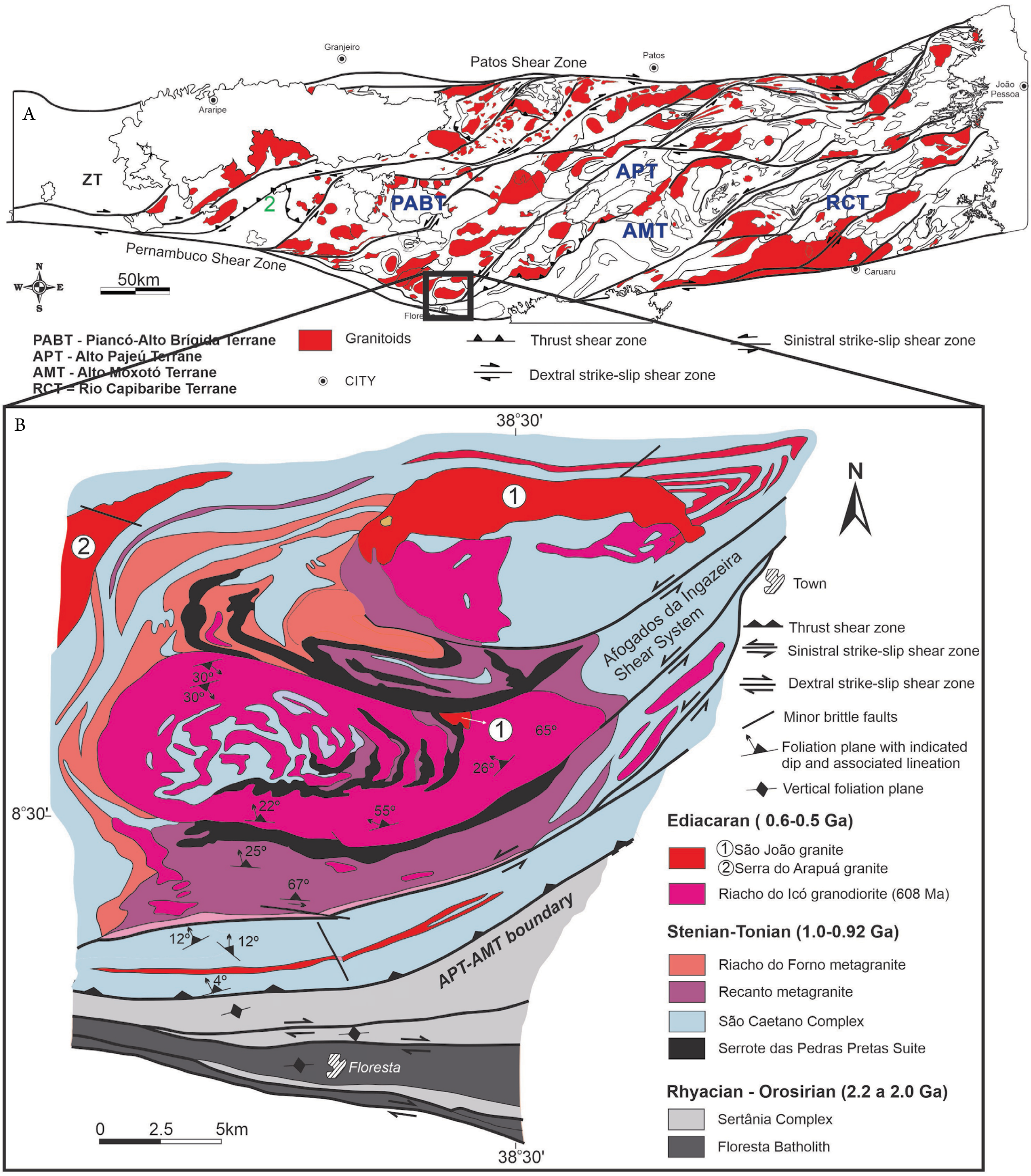

PABT: Piancó Alto Brigida Terrane; APT: Alto Pajeú Terrane; AMT: Alto Moxotó Terrane; RCT: Rio Capibaribe Terrane.

Figure 2. (A) Tectonic sketch of the central subprovince of the Borborema Province following Santos (1995) and Santos & Medeiros (1999); (B) simplified geological map of the Lagoa das Pedras Complex. Figure compiled from Santos (1995) and Lages & Dantas (2016).

Petrography

Point count classification of the studied rocks (50 points from each sample on average) indicates that they correspond to monzogranites and granodiorites (Fig. 4). In samples collected in the inner portions of the intrusion, the hypidiomorphic texture is dominant, however, a granophyric arrangement of crystals might be observed in fine-grained members. A prevalent xenomorphic groundmass occurs in coarse-grained samples, including the porphyritic granites. In the marginal zones, rocks tend to develop mylonitic structures, characterized by K-feldspar rotation and recrystallized quartz crystals, forming ribbons along minor foliation planes composed of bent-flake mica.

The samples are leuco- and mesocratic (color index < 25%) and their main mineralogy include quartz (20–25%), potassium feldspar (microcline and orthoclase, 10–20%), plagioclase (15–25%), greenish- to dark blue hornblende (5%), and biotite (5%). Accessory phases include apatite, titanite, and epidote varieties such as allanite, epidote, and clinozoisite, composing no

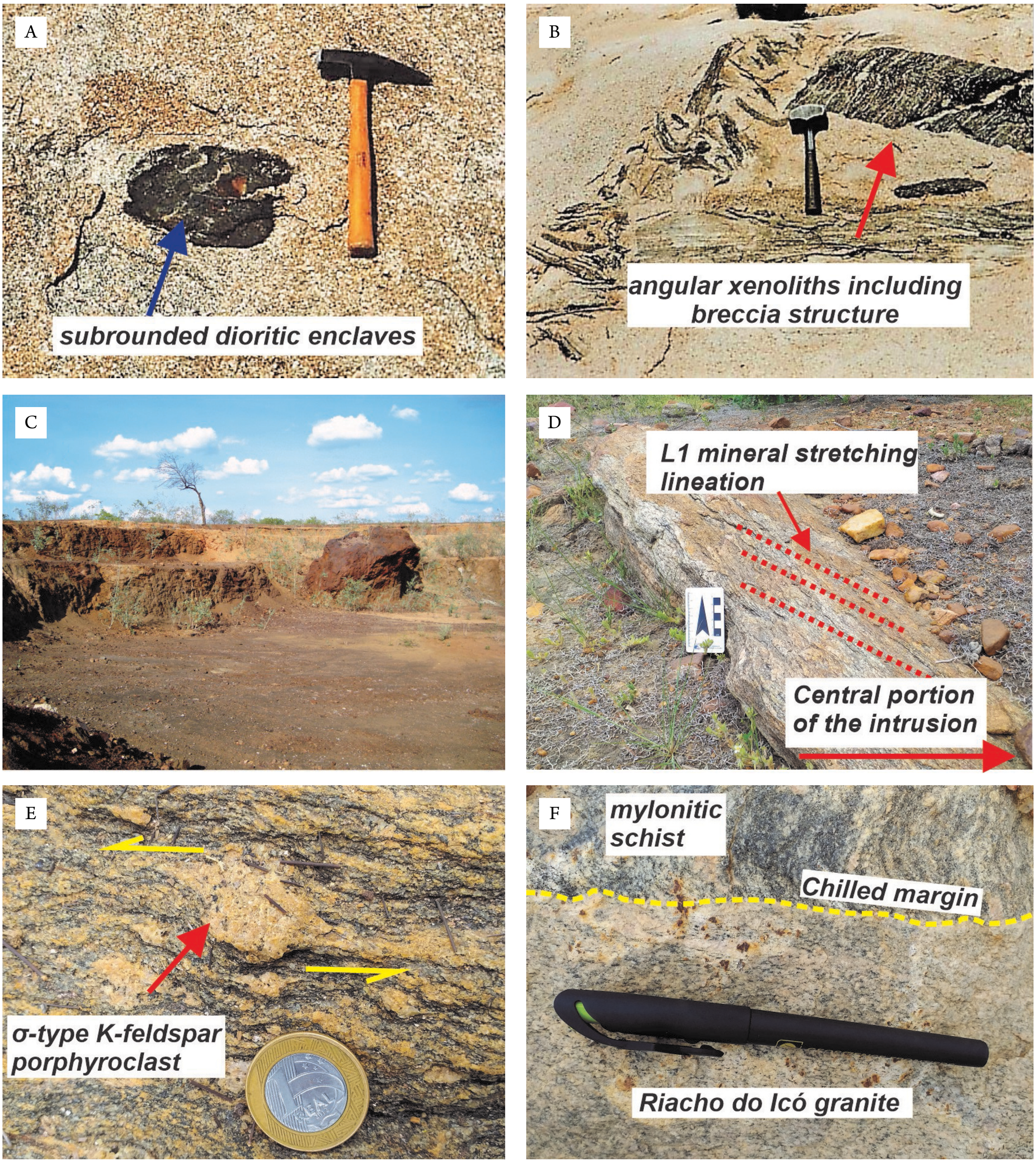

Figure 3. Field relationships of the Riacho do Icó Stock. (A) Subrounded diorite enclave showing injection of felsic material from the host rock. (B) Metric angular xenoliths of the host rock showing a well-developed breccia structure. (C) Hectometric exploited Ti-bearing xenolhitic orebody from the Serrote das Pedras Pretas Suite within the Riacho do Icó Stock. (D) Mineral stretching lineation showing high pitch and dipping toward the central portion of the intrusion. (E) Asymmetrically deformed potassic feldspar porphyroclast showing sinistral movement related to the Afogados da Ingazeira Shear System. (F) Chilled contact between granitic member of the Riacho do Icó Stock and migmatized schist of the São Caetano Complex.

more than 10% of the rock. Chlorite crystals are rare and occur as biotite alteration. Zircon and opaque minerals are generally represented by tiny inclusions in quartz, feldspar or biotite lamellae. Quartz crystals occur as automorphic grains or as polygonal aggregates in deformed marginal zones, often exhibiting undulose extinction. When arranged with stretched biotite, they show clear evidence of magmatic foliation in the micro-scale (Fig. 5A).

Microcline crystals usually exhibit well-developed hatched-twining, whereas film perthite texture is common in orthoclase phenocrysts (Fig. 5B). This mineral also contains several minor inclusions, such as variable-sized subhedral quartz and biotite grains. Plagioclase crystals are mostly subhedral, being classified as oligoclase-andesine. It presents simple Ca-Na zonation, tiny myrmekite intergrowths and moderate degrees of sericitization. Hornblende crystals are mostly subhedral and are generally associated with subhedral to euhedral titanite crystals. They also form elongated aggregates along planar magmatic flow (Fig. 5C).

Allanite exhibits strong zonation as well as inner fractured core, which is an evidence of local metamictization (Fig. 5D). Secondary clinozoisite and epidote occur as products of plagioclase alteration.

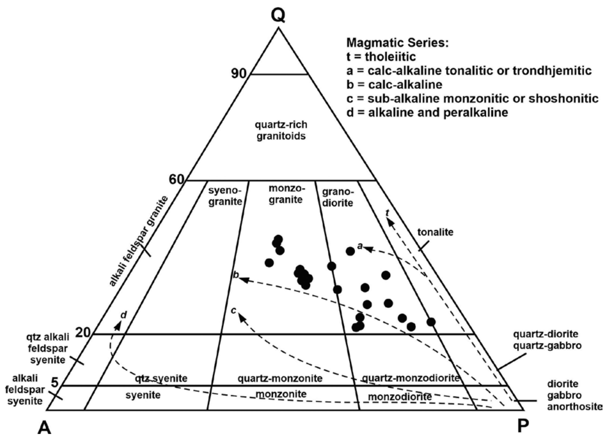

Figure 4. Modal classification of the plutonic rocks of the Riacho do Icó Stock using the Q-A-P triangular diagram from Streckeisen (1976). Magmatic series trends are from Lameyre & Bowden (1982).

ANALYTICAL PROCEDURES

One sample was selected for U-Pb sensitive high-resolution ion microprobe (SHRIMP) analysis at the Research School

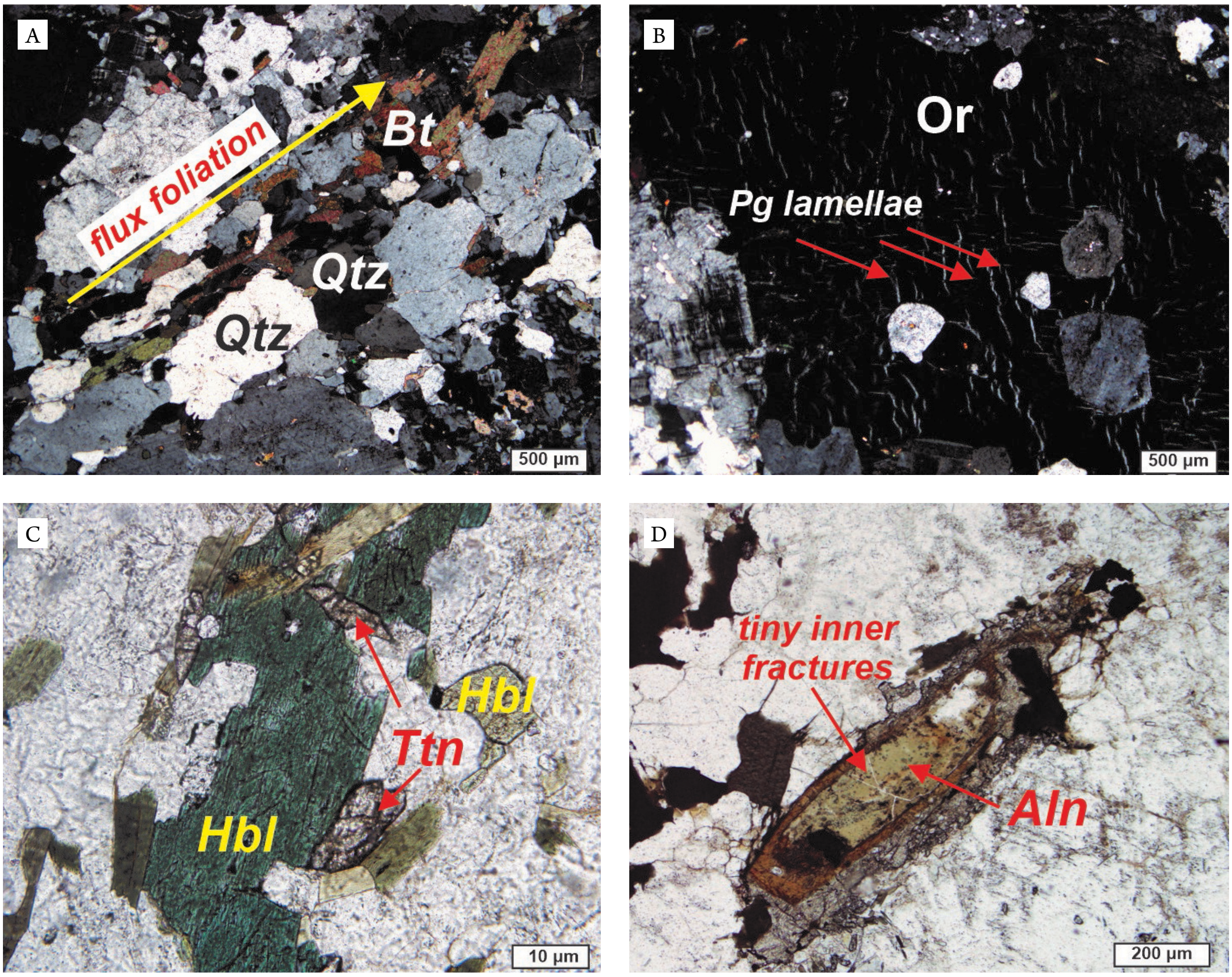

Qtz: quartz; Bt: biotite; Or: orthoclase; Pg: plagioclase; Hbl: hornblende; Ttn: titanite; Aln: allanite.

Figure 5. Photomicrographs of samples of the Riacho do Icó Stock. (A) Anhedral quartz crystals and biotite lamellae oriented along the main magmatic foliation (crossed nicols). (B) Film perthite in subhedral orthoclase phenocryst that also contains minor quartz inclusions (crossed nicols). (C) Subhedral hornblende associated with sub- to euhedral titanite crystals (parallel nicols). (D) Zoned allanite crystal with fractured inner core as the result of metamictization processes (parallel nicols).

of Earth Sciences of the Australian National University. It was polished and characterized through various image types, including visual and back-scattered, being coated with a conductive material to avoid sample charging. All analyses were guided by previously obtained cathodoluminescence images in order to obtain information about the inner structures of the zircon crystals. The standard used was the FC1 (1099 Ma; Paces & Miller 1993). A detailed analytical procedure used in this analysis can be found in Williams (1998) and Stern (1997). Data were reduced in Isoplot 4.5 (Ludwig 2012).

For the geochemical investigation, twelve samples were selected, avoiding those with evidence of deformation and alteration, and then analyzed for major and trace element distributions at the GEOSOL and NEG-LABISE laboratories in Brazil. Oxides of major elements were determined using a Varian Vista Pro Inductively Plasma Atomic Emission Spectrometer (ICP-AES) as well as an X-Ray Fluorescence Rigaku ZSX Primus II spectrometer. Trace elements were determined via Perkin-Elmer Sciex ELAN 6000 inductively coupled plasma mass spectrometer (ICP-MS). Analytical precision was 1–5% for major oxides and ± 10% for trace elements. The selected geochemical diagrams were acquired in the GCDkit software (Janoušek *et al.* 2006) and by in-house reproduced excel spreadsheets.

U-Pb GEOCHRONOLOGY

The Sample ES-15 was selected for U-Pb SHRIMP zircon determinations and corresponds to a hornblende-biotite granodiorite that lacks any evidence of tectonic deformation (geographical coordinates 8º28'27"S and 38º35'41"W). Analytical determinations are presented in Table 1. Zircon crystals from this sample are euhedral, mostly translucent, and form 80–220 µm elongated prisms. Their axial ratios range between 2:1 and 5:1 and they present well-developed oscillatory zoning. Also, rim overgrowths are widespread (Fig. 6A).

U and Th contents of the analyzed zircon crystals are wide ranged, *i.e.* between 49 and 1,049, and 1 and 1,045 ppm, respectively. Three groups of zircon crystals were identified. The first is composed of crystals that show strongly developed oscillatory zoning and present Th/U ratios higher than 0.1. They yielded a Concordia age of 607 ± 3 Ma (Fig. 6B), which is interpreted as the crystallization age of the granodiorite.

On the other hand, several spots were conducted in crystals with recrystallization rims that are characterized by very low Th/U ratios. They yield a Concordia age of 600 ± 8 Ma (Fig. 6C), which probably represents a local metamorphic event, such as migmatization, once that it is coeval to the interpreted magmatic ages. Three crystals (not plotted) are slightly older, presenting ages at around 950 Ma (#17.3, 13.2, and 6.2), which are interpreted as an inheritance of host rocks.

WHOLE-ROCK GEOCHEMISTRY

In the studied samples, major element distribution is homogeneous (Tab. 2). They present high SiO_2 (66.5–71.9 wt%) and Al_2O_3 (13.8–15.9 wt%), moderate Na_2O (4.09–4.74 wt%) and K_2O (3.75–4.38 wt%) and low contents of CaO (1.86–2.56 wt%), Fe_2O_3 (1.98–3.45 wt%), and MgO (0.61–1.14 wt%). This pattern is reflected in the R1-R2 diagram from De la Roche *et al.* (1980), where samples plot in the granite and granodiorite fields (Fig. 7A), which is in accordance with the petrographic modal count. On the SiO_2 *vs.* $Na_2O + K_2O - CaO$ diagram from Frost *et al.* (2001), the samples correspond to calc-alkalic granites, with three samples plotting on the alkali-calcic field (Fig. 7B). On the SiO_2 *vs.* FeOt(FeOt + MgO) diagram from Frost *et al.* (2001), they plot in the magnesian field, sharing similarities with Cordilleran related-granites (Fig. 7B) and metaluminous magmas (Fig. 7D), based on the $Al_2O_3/(Na_2O + K_2O)$ *vs.* $Al_2O_3/(CaO + Na_2O + K_2O)$ molar diagram modified by Maniar & Piccoli (1989).

Table 1. Summary of U-Pb sensitive high-resolution ion microprobe (SHRIMP) data of zircon grains from sample ES-15.

Grain Spot	% $^{206}Pb_c$	ppm U	ppm Th	$^{232}Th/^{238}U$	ppm $^{206}Pb^*$	(1) $^{206}Pb/^{238}U$ Age	(1) $^{207}Pb/^{206}Pb$ Age	% Discordant	(1) $^{207}Pb^*/^{206}Pb^*$	±%	(1) $^{207}Pb^*/^{235}U$	±%	(1) $^{206}Pb^*/^{238}U$	±%	errcorr
1.3	0.03	540	29	0.06	46.1	610.6	616	1	0.06034	0.7	0.827	1.4	0.0994	1.2	.872
4.2	0.00	329	314	0.99	28.2	613.4	631	3	0.06078	1.1	0.837	1.6	0.0998	1.1	.695
5.2	0.77	621	482	0.80	52.6	600.8	621	3	0.0605	2.5	0.814	2.7	0.0977	1	.386
6.2	0.26	154	86	0.58	17.9	817.5	943	13	0.07049	1.4	1.314	1.8	0.1352	1.2	.648
6.3	0.00	554	19	0.04	54.2	694.2	695	0	0.06262	0.7	0.982	1.3	0.1137	1.1	.836
7.2	0.51	538	14	0.03	43.6	577.5	598	3	0.05984	1.4	0.773	1.8	0.09372	1	.597
8.2	2.61	771	1,045	1.40	64	579.6	591	2	0.0596	4.7	0.774	4.9	0.0941	1.1	.220
13.2	--	190	103	0.56	23.1	854	996	14	0.07237	1.1	1.414	1.6	0.1417	1.1	.726
13.3	2.73	1,049	44	0.04	83.1	553.7	564	2	0.0589	4.8	0.729	5	0.08969	1.1	.214
14.2	0.13	387	35	0.09	32.5	600.5	630	5	0.06073	0.94	0.817	1.4	0.0976	1.1	.749
15.2	0.19	337	34	0.10	29.1	615.8	631	2	0.06078	1.1	0.84	1.6	0.1002	1.1	.686
17.1	--	123	47	0.40	17.4	983	991	1	0.07218	1.1	1.639	1.7	0.1647	1.2	.725
18.1	0.00	49	1	0.01	4.05	586.6	598	2	0.0598	2.3	0.786	2.8	0.0953	1.6	.557
19.1	0.00	246	10	0.04	21.1	614.7	618	1	0.06041	1	0.833	1.5	0.1	1.1	.731
19.2	0.21	617	27	0.05	51.8	600.2	608	1	0.06011	1.2	0.809	1.6	0.0976	1	.654
20.1	0.27	858	42	0.05	72.9	606.6	607	0	0.06008	0.92	0.817	1.4	0.0987	1	.744

*corrected common lead accordingly.

The chondrite-normalized (Nakamura 1974) spidergram for the samples displays moderate to high values of Large Ion Lithophile Elements (LILE) and low contents of High-Field Strength Elements (HFSE). This is reflected on positive peaks of Rb, K, and Ba and negative anomalies of Nb, P, Ti, and Y (Fig. 8A). Figure 8B displays the chondrite-normalized (Sun & McDonough 1989) Rare Earth Element (REE) patterns of the studied rocks, which are characterized by moderate to strong fractionation between light and heavy REE ($[La/Yb]N = 30–113$) and lack Eu anomalies ($Eu/Eu^* = 0.80–0.91$). Based on the Y *vs.* Nb tectonic discriminating diagram, the studied samples represent products of volcanic arcs and collisional settings (Fig. 9).

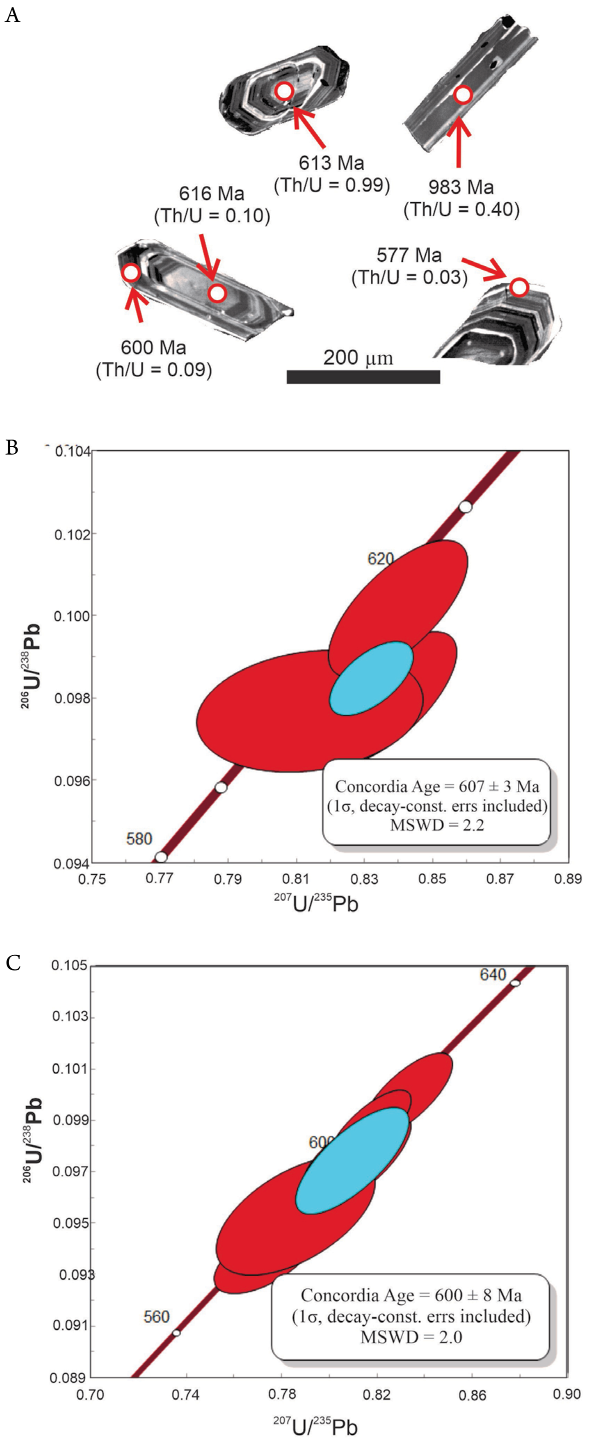

SHRIMP: sensitive high-resolution ion microprobe.

Figure 6. (A) Cathodoluminescence images of representative zircon grains from sample ES-15; (B) U-Pb SHRIMP zircon ages of crystals with Th/U ratios higher than 0.1 from sample ES-15; (C) U-Pb SHRIMP zircon ages of crystals with Th/U ratios lower than 0.1 from sample ES-15.

DISCUSSION

Magma emplacement

Due to the variety of contrasting geological features of the Riacho do Icó Stock, they might bring out distinct hypotheses for magma emplacement, which has already been partially discussed by Santos (1995) and even now, still needs further investigations. For instance, as commonly invoked to explain plutonic injection in middle to upper crustal levels in several orogenic belts worldwide (*e.g.*, Cruden 1990), part of the Riacho do Icó parental magma might represent buoyant material that formed via diapirism, forcing host/wall supracrustal and adjoining metaplutonic rocks upward. The main evidence for this hypothesis include:

- roughly rounded to ellipsoidal shape of the intrusion;
- deviation of the host-rocks foliation;
- low-angle tectonic foliation and high-pitch down-dip lineation that converge to the center of the intrusion.

Such a model has been widely used to explain the famous “space problem” of granites, especially in post-orogenic conditions (*e.g.*, Bateman 1989). A clear problem faced in our case is that the 607 Ma age put this intrusion in a syn-collisional/contractional regime (*e.g.*, Brito Neves *et al.* 2003, Weinberg *et al.* 2004, Ganade de Araújo *et al.* 2014c, Sial & Ferreira 2016) instead of in a post-orogenic stage.

Nonetheless, the presence of several metric-scale xenoliths of different host rock types, including mafic-ultramafic bodies and those that exhibit breccia structure are widespread throughout the Riacho do Icó Stock. The xenoliths present tabular, rounded to irregular shapes that may be concordant to the intrusion magmatic foliation, also presenting remnants of early deformation stages. Evidence of a mixed population of xenoliths and stepped contacts between the granite and host/wall rocks suggests a component of crustal stopping, in which the roof collapse by crustal subsidence would explain forceful magmatic injection (Glazner & Bartley 2006, Žák & Paterson 2006).

In spite of local granitic sheets related to thrust tectonics verging top-to-the south that are present throughout the Alto Pajeú Terrane, from the central portion of the intrusion to its marginal zones, well-developed magmatic flux is progressively transposed by strike-slip foliation, especially in its southern margin. It has been long recognized that transcurrent shear zones might act as important sites of crust dilatation and magma percolation (Tikoff & Teysser 1994), including examples from the Borborema Province (*e.g.*, Vauchez *et al.* 1995, Viegas *et al.* 2013, Lima *et al.* 2017). Also, tectonic foliation is associated to well-developed sub- to horizontal mineral and stretching lineations, which might be solely the result of stress rotation or may suggest shallow lateral magma propagation from the feeder zone

Table 2. Major elements composition (wt.%) and trace elements (ppm) of samples of the Riacho do Icó Stock.

Sample	Major elements (wt. %)											
	RI01	RI02	RI03	RI04	RI05	RI06	RI07	RI08	RI09	RI10	RI11	ES15
SiO_2	71.9	65.86	65.7	68.8	68.2	71.2	67.26	69.93	70.3	67.25	71.3	71.3
TiO_2	0.32	0.61	0.54	0.52	0.34	0.41	0.47	0.38	0.45	0.47	0.41	0.33
Al_2O_3	13.8	14.85	15.9	14.7	14.86	15.1	14.68	14.49	15.3	14.94	14.7	14.1
Fe_2O_3(total)	2.10	3.45	3.17	2.90	1.98	2.50	2.77	2.19	2.68	2.92	2.58	2.17
Cr_2O_3	0.03	0.04	0.03	0.02	0.02	0.03	0.04	0.03	0.03	0.03	0.02	0.02
MnO	0.01	0.03	0.03	0.02	0.02	0.02	0.03	0.03	0.02	0.03	0.02	0.01
MgO	0.69	1.16	1.07	1.14	0.62	0.90	0.84	0.67	0.96	0.92	0.90	0.76
CaO	1.86	2.56	2.55	2.50	2.02	2.51	2.31	1.91	2.44	2.36	2.31	2.03
Na_2O	4.09	4.74	4.72	4.32	4.29	4.37	4.36	4.35	4.53	4.58	4.48	4.29
K_2O	3.91	3.93	3.75	3.96	4.38	4.00	4.13	3.91	4.38	3.97	3.91	4.05
P_2O_5	0.16	0.17	0.15	0.17	0.1	0.16	0.15	0.1	0.16	0.15	0.17	0.12
LOI	0.64	1.54	1.24	0.61	1.07	0.68	1.42	0.62	0.75	0.70	0.73	0.53
Total	99.5	98.9	98.85	99.7	99.0	101.8	98.5	98.6	102.0	98.3	101.5	99.7
	Trace elements (ppm)											
V	24	39	63	45	16	38	42	43	37	41	48	36
Co	6.2	9.5	7.4	9	5.2	7.7	8.1	6	8.7	8.2	7.9	6.1
Ni	12	17	14	16	10	13	15	13	14	15	17	19
Cu	5	11	9	10	< 5*	12	10	< 5*	14	12	10	< 5*
Tl	3.1	2	1.2	1.1	0.9	0.7	0.7	0.7	0.6	< 0.5*	< 0.5*	< 0.5*
Zn	96	95	95	103	79	96	86	84	87	89	94	103
Ga	26.1	26.3	23.4	28.5	28.1	24.5	24	25.6	25.7	25.1	25.5	27.3
Rb	166.5	153	126.5	162.7	172.1	118.8	121.4	157.7	127.5	117.4	120.3	170
Sn	2.4	2.5	2	2.9	1.7	1.8	1.6	1.4	1.8	1.7	1.8	2.1
Sr	421	604	677	626	487	648	650	435	649	630	631	429
W	11.6	11.7	8	6.5	8.3	9.6	14.5	10.3	11.8	10.2	9.8	8.6
Zr	157	198	188	181	136	156	158	154	173	149	147	152
Nb	10.6	13.79	7.99	10.4	6.67	7.59	8.57	6.59	8.24	7.94	7.51	6.83
Cs	6.82	6.99	5.80	7.59	5.45	3.49	3.39	3.59	3.59	6.31	6.46	2.34
Ba	749	1184	1218	1292	873	1257	1320	727	1248	1086	1127	741
La	32.5	29.5	22.5	42.1	22.1	18.5	20.4	51	33.1	31.6	31.4	46.1
Ce	56	70	50.3	77.5	40.5	40.9	42.3	55.1	61.9	57.8	55.5	55.3
Pr	7.3	7.18	5.71	9.78	4.79	4.41	4.71	9.46	7.26	6.71	6.5	8.26
Nd	25.9	27.2	21.7	36.3	18.1	16.7	18.7	34.8	27.7	25.2	24.3	30.2
Sm	4.2	5.1	4.1	6.5	3.4	3.7	3.9	5.2	4.8	4.3	4.4	4.8
Eu	0.89	1.31	1.01	1.48	0.79	0.94	1.02	1.11	1.16	1.07	1.07	1.01
Gd	2.45	3.88	2.91	4.58	2.46	2.84	2.87	3.29	3.36	3.24	3.2	3.11
Tb	0.26	0.47	0.36	0.52	0.24	0.34	0.35	0.31	0.41	0.36	0.36	0.3
Dy	1.08	2.32	1.61	2.34	0.95	1.51	1.53	1.11	1.74	1.57	1.42	1.12
Ho	0.17	0.37	0.25	0.35	0.15	0.21	0.24	0.17	0.25	0.26	0.24	0.16
Er	0.45	0.97	0.64	0.87	0.33	0.58	0.63	0.40	0.63	0.65	0.57	0.38
Tm	0.07	0.13	0.08	0.11	< 0.05*	0.08	0.07	< 0.05*	0.08	0.08	0.07	< 0.05*
Yb	0.4	0.8	0.5	0.7	0.3	0.4	0.5	0.3	0.5	0.5	0.4	0.3
Lu	0.05	0.11	0.06	0.10	0.05	0.06	0.07	0.05	0.05	0.07	0.07	0.05
Y	4.2	9.27	6.42	9.36	3.8	6.14	6.43	4.79	7.08	6.72	6.26	4.54
Hf	5.55	6.06	4.33	5.69	4.75	4.59	4.62	4.88	5.36	4.71	4.6	5.1
Ta	3.03	2.36	1.66	1.53	0.98	0.97	0.97	0.74	0.95	0.8	0.79	0.51
Th	9.3	11.1	7.7	10.5	7.2	7.8	8.1	7.9	9.4	8.4	7.6	7.3
U	2.28	2.63	2.04	2.62	2.02	1.49	1.61	2.32	1.78	1.65	1.61	2.19
SREE	131.72	149.34	111.73	183.23	94.11	91.17	97.29	162.25	142.96	133.41	129.48	151.04
Eu_N/Eu^*	0.85	0.91	0.90	0.83	0.84	0.89	0.94	0.82	0.89	0.88	0.88	0.80
$(La/Yb)_N$	54.1	24.5	30.0	40.1	49.1	30.8	27.2	113.3	44.1	42.1	52.3	102.4
$(La/Sm)_N$	4.76	3.56	3.38	3.98	4.00	3.08	3.22	6.03	4.24	4.52	4.39	5.91
$(Gd/Yb)_N$	4.8	3.86	4.64	5.22	6.55	5.65	4.58	8.76	5.36	5.17	6.37	8.29

Below detection limit. Total iron reported as Fe_2O_3. N-Chondrite-normalized rare earth elements (Nakamura 1974). Where Eu is $\sqrt{[(Sm_N \times Gd_N)]}$.

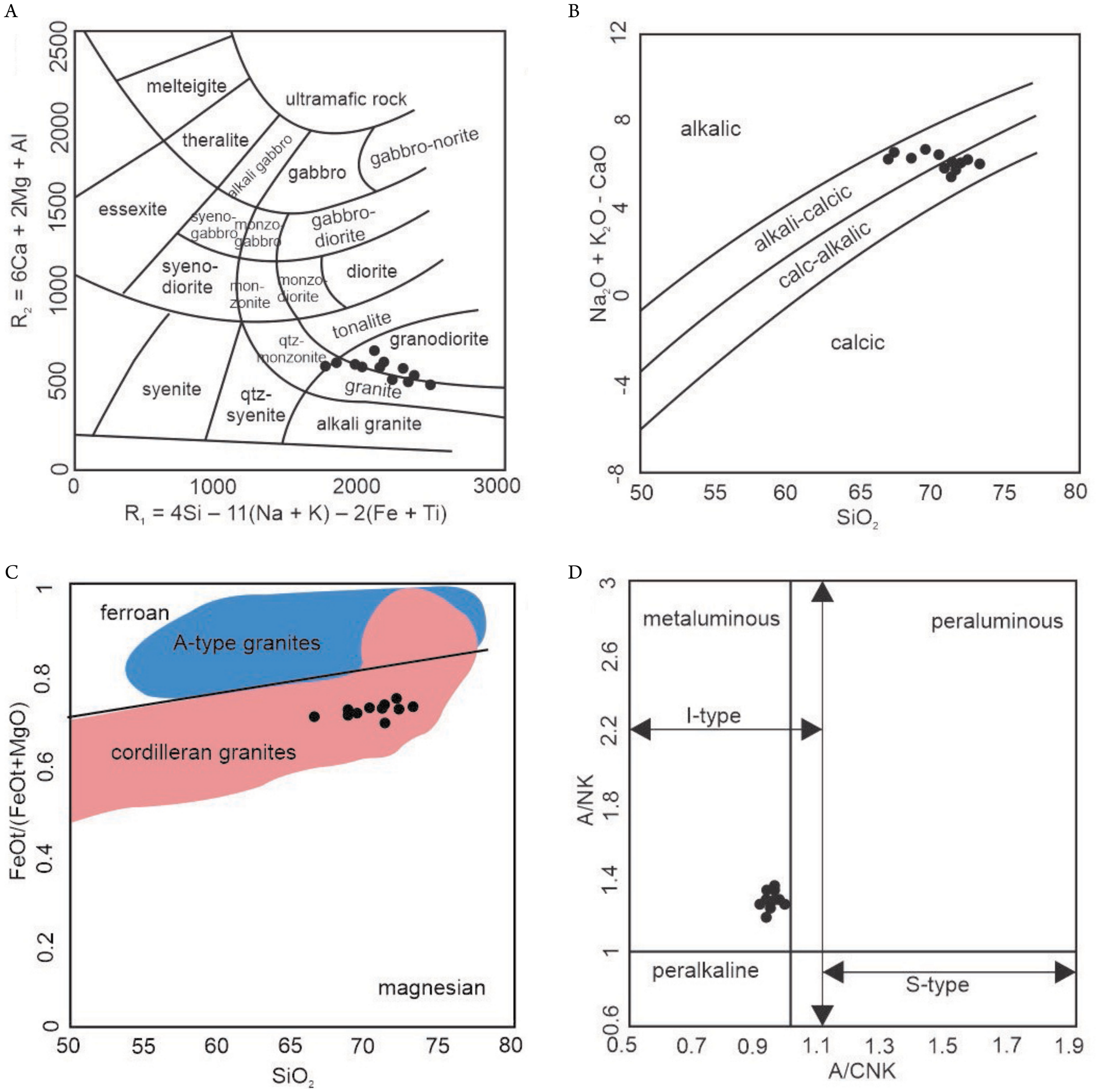

Figure 7. Geochemical characteristics of samples from the Riacho do Icó Stock. (A) R1-R2 diagram (De la Roche *et al.* 1980); (B) $SiO_2 + Na_2O + K_2O$ = CaO diagram (Frost *et al.* 2001); (C) FeOt/(FeOt + MgO) diagram (Frost *et al.* 2001); (D) A/CNK vs. A/NK diagram (Maniar & Piccoli 1989).

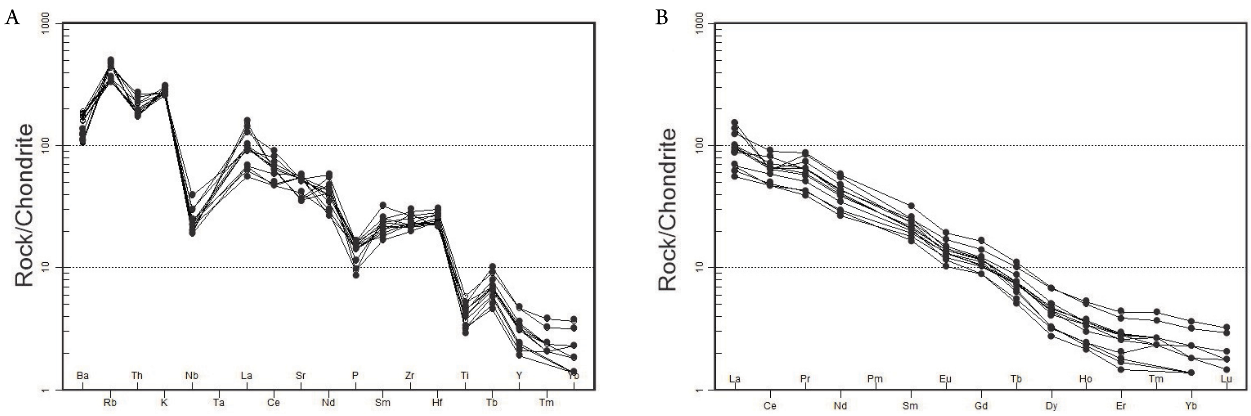

Figure 8. Trace element distribution on samples of the Riacho do Icó Stock. (A) Spidergram normalized to the Chondrite of Nakamura (1974); (B) rare Earth elements (REE) distribution diagram normalized to the Chondrite of Sun & McDonough (1989).

during its ascent, which is typical from laccolith-type intrusions (*e.g.*, Petford *et al.* 2000, Gutiérrez *et al.* 2018).

In the western Borborema Province, *en cornue* plutons are clear indicators of shear-zone control and a direct result of synkinematic pluton emplacement (Weinberg *et al.* 2004). In an ideal model, this mechanism involves changes in the rheological properties of rocks adjoining shear zones, creating fragile, dilational, low-mean-pressure triple points into which ascending magmas intrude, giving rise to plutons (Cruden & Weinberg 2018). Another example of *en cornue* granites older than 600 Ma is the ~650 Ma Tavares Batolith of the Piancó-Alto Brígida Fold Belt (Brito Neves *et al.* 2003, Weinberg *et al.* 2004). It suggests that the transcurrent regime might precede other accepted ages for lateral movements in the province (*i.e.* ~560 Ma, Viegas *et al.* 2014), but still lacks regional significance.

Based on the presented data, we suggest that hybrid mechanisms might have acted during the Riacho do Icó magma emplacement, involving forced intrusion, roof collapse and coeval shearing in a possible fossil deep-seated discontinuity that might have been triggered in a triple point from the Pernambuco and Afogados da Ingazeira Shear Systems. In such a model, crustal space would be generated between crustal step-overs and oblique shearing (Fig. 10), which has been already described in several deformed orogenic belts worldwide (Hutton 1988 and references therein). It is important to notice that the described shear system might have been associated to pull-apart tectonics to create crustal space. Such structures coincide with regional geophysical lineaments that present strong density gradients as well as magnetic susceptibility, representing a possible terrane boundary (Oliveira & Medeiros 2018).

Magma source and tectonic setting

Samples of the Riacho do Icó Stock present granitic to granodioritic compositions and the U-Pb zircon dated sample via SHRIMP methodology yielded a crystallization age of 607 ± 3 Ma, which is coeval to abundant magmatism related to the Brasiliano Orogeny in South America (Brito Neves *et al.* 2014). Associated rocks present major geochemical characteristics compatible with Cordilleran magmas that crystallized as I-type granites. The presence of modal hornblende and biotite as well as the color index, support these interpretations. Flame/film perthites observed in the studied samples are particularly well-developed in coarse-grained members, being generally interpreted as subsolidus magmatic exsolution that reflects systematic replacement reactions between Na-K and Ca-K during two-feldspar crystallization (Yuguchi & Nishiyama 2008).

The chondrite normalized trace-element spidergram shows evident enrichment of LILE and depletion of HFSE, including negative anomalies of Nb, P, and Ti. Such a pattern might be explained by Ti-rich phases controlling the partition coefficient of these elements in the source region, such as rutile, titanomagnetite, and sphene (Foley *et al.* 2000). REE distribution shows moderate to high fractionation, in which low contents on heavy REE may reflect the presence of garnet or amphibole in the melt residuum, whilst the lack of evident negative Eu anomalies suggest an absence of plagioclase fractionation and high oxygen fugacity (fO_2). In addition, the discrete Ce anomaly would reflect the incorporation of pelagic sediments and seawater in the source region (Neal and Taylor 1989).

The distribution of trace elements is compatible with magmas generated in modern-like subduction zones (Gill 1981, McMillan *et al.* 1989, Klemme *et al.* 2006). Arc-related

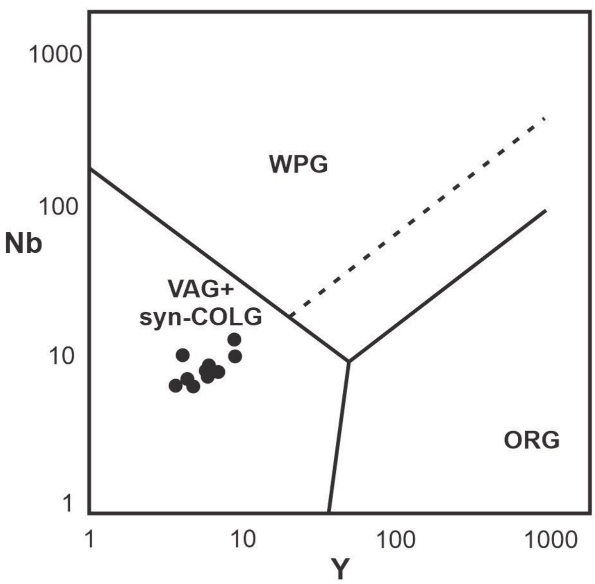

Figure 9. Y vs. Nb tectonic setting discriminating diagram for samples of the Riacho do Icó Stock.

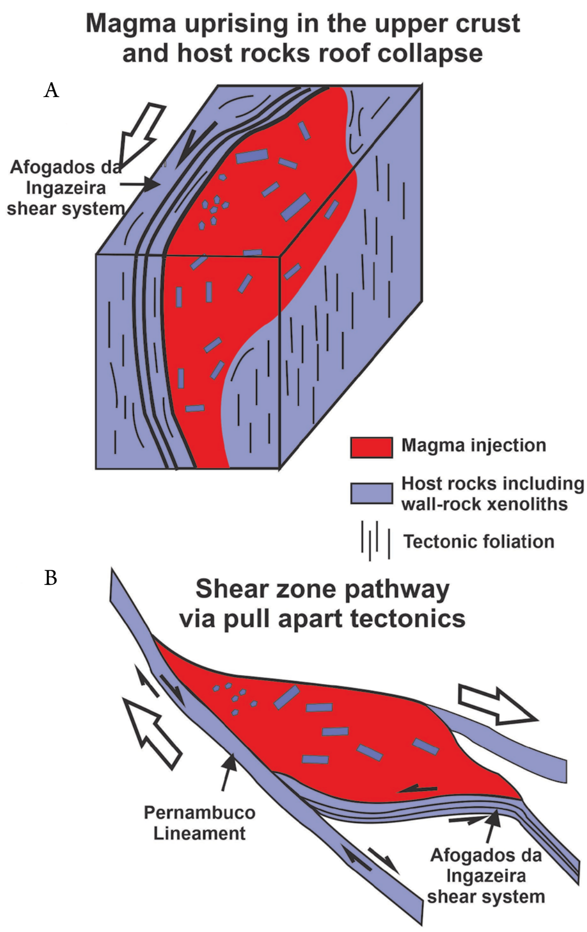

Figure 10. Proposed emplacement model for the Riacho do Icó Stock, involving (A) magma ascent and stopping, (B) followed by transtensional tectonics related to the regional shear zones.

magmas tend to result from upper mantle melting followed by fractional crystallization during emplacement in the crust (Sisson & Grove 1993). Despite that, it might only reflect the source characteristics, the interpretation of "arc-related" magmatism for the Riacho do Icó intrusion is also supported by plots on the discriminating diagram of Pearce *et al.* (1984).

Specific geochemical aspects of rocks from the Riacho do Icó stock, including high SiO_2, Na_2O, and Ni contents are commonly ascribed to plutonic and volcanic rocks derived from adakitic magmas. In their definition of adakite and related rocks, Defant & Drummond (1990) gave strong emphasis on the characteristic high Sr and low Y contents of these magmas, reflecting high Sr/Y (avg. 100) ratios, which is unusual in "normal" arc-related magmas, being a distinctive feature. This pattern is seen in samples of the Riacho do Icó Stock (Fig. 11A). Also, Martin *et al.* (2005) proposed that adakites might be grouped as Low-Silica (LSA) and High-Silica groups (HSA), and we suggest that our samples correspond to the latter (Fig. 11B).

Adakitic melts might be generated in a number of tectonic settings, including pristine products of slab melting during hot subduction, and consequently, upper mantle melting has a minor influence on magma generation (Castillo 2012 and references therein). In addition, distinct stages of ongoing subduction might also generate adakite-like magmas, including convergent termination (Sajona *et al.* 1996), collisional settings (Sajona *et al.* 2000), slab detachment (Gao *et al.* 2007), and ridge subduction (Tang *et al.* 2010). In addition, MgO wt%. has been used as a source marker, since this oxide is usually controlled by deep-seated phases. On the SiO_2 *vs.* MgO diagram proposed by Martin *et al.* (2005), samples from the Riacho do Icó Stock are akin to adakites formed by slab melting (Fig. 11C), which is coherent with the HSA group proposal.

The identification of pure adakites is known to be difficult and, especially in Precambrian and strongly deformed regions such as the Borborema Province, it should be taken with caution, since several processes including Assimilation-Fractional Crystallization (AFC) might lead to a wide range of rocks that present similar characteristics (Castillo 2012). However, based on the data presented herein, it is suggested that subduction stages of the Brasiliano orogeny might have involved some degree of melting of a metamorphosed basaltic slab in deep-seated regions (garnet-bearing source) during early Ediacaran convergence or an underplated arc basalt source. This assumption is reinforced by the close spatial association with the SPP Suite that record high-grade metamorphism (eclogitic facies) at 625 Ma and could mark the transition between subduction to a syn-collisional regime (Lages & Dantas 2016). Lastly, it is pointed out that our interpretations represent the first attempt to test such a petrogenetic hypothesis for granitic rocks within the Alto Pajeú Terrane and must further be tested and expanded to other stocks and batholiths.

Regional Constraints

The Brasiliano-Pan African Orogeny was the major tectonic event that built-up the South American Neoproterozoic provinces, resulting from collisional episodes between major cratonic blocks (Brito Neves *et al.* 2000). Crustal collage occurred in four major intervals:

- 800–740 Ma;
- 660–610 Ma;
- 590–560 Ma;
- 520–500 Ma (Brito Neves *et al.* 2014).

In the Borborema Province, early magmatism related to accretion tectonics is recorded in the northern subprovince, represented by the Tamboril-Santa Quitéria arc-system (Santos *et al.* 2008). In this orogenic complex, long-lived magmatism

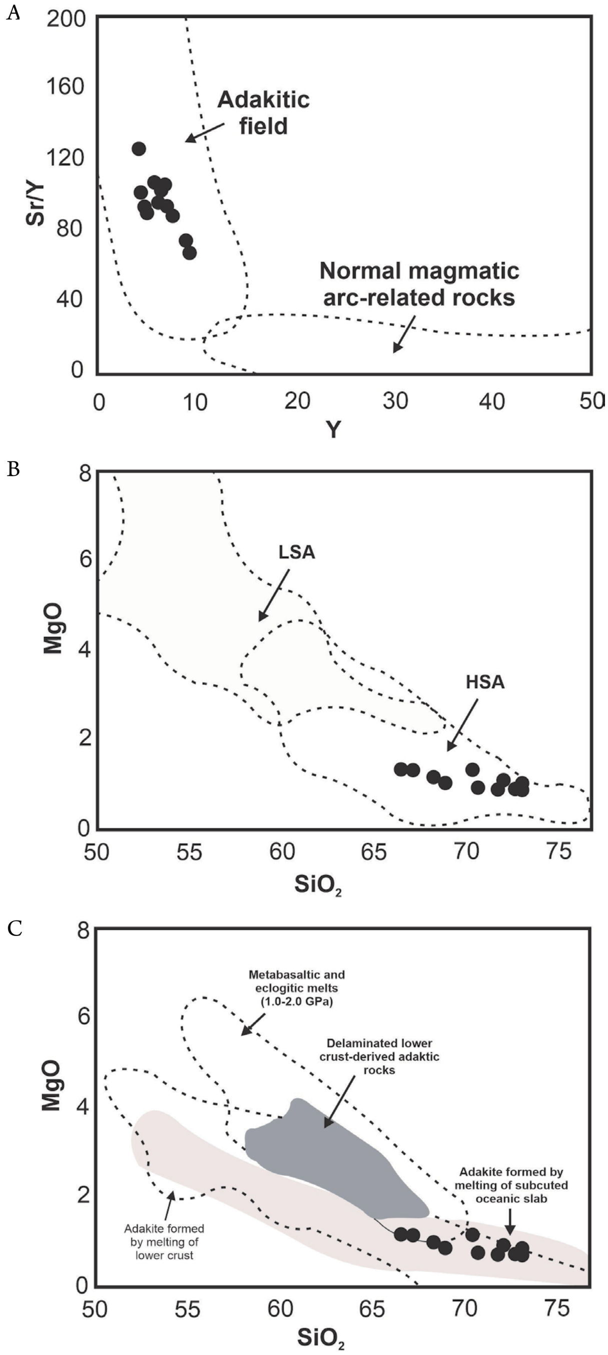

Figure 11. Plots of samples from the Riacho do Icó Suite: (A) Sr/Y diagram with fields of adakites and "normal" calc-alkaline rocks from Defant & Drummond (1990). (B) MgO vs. SiO_2 diagram discriminating high-silica groups (has) and low-silica (LSA) from Martin *et al.* (2005). (C) MgO. vs. SiO_2 diagram discriminating sources for adakitic magmas with fields/data compiled from Rapp *et al.* (1999, 2002), Sen & Dunn (1994), Rapp & Watson (1995), Skjerlie & Patiño Douce (2002), and Wang *et al.* (2006).

comprises a juvenile arc that evolved to a mature stage between ca. 880–660 Ma, followed by a final stage of crustal anatexis at ca. 615–600 Ma (Ganade de Araújo *et al*. 2014a).

In contrast, other domains of the Borborema Province, including the Alto Pajeú Terrane, present magmatic activity related to the Brasiliano orogeny ranging from 650 to 550 Ma (Sial 1990). Despite discrete differences on geochemical and isotopic aspects of the vast number of granites described in the central subprovince, they can be grouped as follows:

- normal to high-K calc-alkaline granites dated at c. 640–600 Ma;
- high-K calc-alkaline and shoshonitic granites dated at 590–580 Ma;
- post-collision alkaline granites dated at c. 570 Ma;
- anorogenic granites aged at c. 540–510 Ma (Guimarães *et al*. 2004).

A similar subdivision is presented by Sial & Ferreira (2016). Based on the geochronological determinations obtained in this study, the Riacho do Icó Stock fits with the first group and thus would be related to a final stage of the first episodes of the Brasiliano tectono-magmatic activity. Granites of this group are generally related to flat-lying foliation related to thrust tectonics due to initial plate motion (Guimarães *et al*. 2004, Archanjo *et al*. 2008).

Based on the proposed emplacement model for the Riacho do Icó Stock, which is closely related to the Afogados da Ingazeira Shear System, it is possible that early strike-slip movements (and progressive transition from thrust to lateral tectonics) might have resulted from lateral escape or extrusion tectonics, that can lead to local magma percolation along major crustal discontinuities, including reactivated suture zones (*e.g.*, Tapponnier *et al*. 1982). If this was the case, the Riacho do Icó Stock would be related to the continental collision of the Amazonian-West Africa Craton and the Paleoproterozoic basement of the Borborema Province, which is interpreted as a first Neoproterozoic collisional stage in the province (Ganade de Araújo *et al*. 2014c).

It has been proposed that a wide magmatic arc was formed in the northernmost portion of the central subprovince (Piancó Alto Brigída Terrane/Fold Belt), presenting several stages of magma generation covering early calc-alkaline granites that evolved to post-collisional magmas, *i.e.* from 635 to 580 Ma (Brito Neves *et al*. 2016). Based on our investigation and on a number of papers published on the central Borborema Province (*e.g.*, Santos & Medeiros 1999, Guimarães *et al*. 2004, 2011, Lages *et al*. 2016, Lima *et al*. 2017), we suggest that the Riacho do Icó Stock might be part of this continental magmatic arc, that would be extended to the Alto Pajeú Terrane and that it represents a disjoint fragment of crust dislocated by transcurrent movements, which are one of the most remarkable characteristics of the Central Subprovince of the Borborema Province.

CONCLUSIONS

- The Riacho do Icó Stock corresponds to perthitic biotite-amphibole monzogranites and granodiorites that represent the largest Ediacaran plutonic exposure of the Riacho das Pedras Complex of the Alto Pajeú Terrane. It is dated at ca. 607 Ma, which represents the age of the rock crystallization. Coeval and local metamorphism is marked by ca. 600 Ma aged overgrowth zircon crystal rims;
- Field evidence suggests that hybrid mechanisms took place during magmatic ascent. They include a widespread and heterogeneous population of angular xenoliths, host-rock foliation deviation, and the development of mylonitic members at the intrusion rims. We suggest that the crustal discontinuity magma flow (progressive deformation, intrusion shape and close relationship with sinistral shear zones) in a triple point generated step-overs and crustal space along the Afogados da Ingazeira System, marking local extensional sites during plate convergence.
- Whole-rock geochemistry suggests that the Riacho do Icó magma was generated in a transitional setting between late orogenic and syn-collisional conditions. In addition, it is also suggested that slab melting might have been involved in the source region, despite the classical upper mantle origin suggested for classical calc-alkaline arc magmas in the central subprovince. Lastly, based on the obtained geochronological determinations, it is possible that the Riacho do Icó Stock belongs to the long-lived magmatic arc proposed in the central subprovince, representing a dismembered fragment within the Alto Pajeú Terrane.

ACKNOWLEDGMENTS

This paper is kindly dedicated to the memory of Edilton José dos Santos, known as "professor". The Riacho do Icó Stock represents one of his many geological curiosities and the authors are pleased for the opportunity to add information on the knowledge of the Borborema Province granites. Part of the geochemical data was obtained in the NEG-LABISE laboratory and we kindly appreciate the lab staff. We would like to thank Alcides Sial, Valderez Ferreira and Claudio Riccomini for the opportunity and the reviewers for their suggestions. This research was funded by the National Institute of Science and Technology for Tectonic Studies (INCT), Brazil.

ARTICLE INFORMATION

Manuscript ID: 20190127. Received on: 08/31/2019. Approved on: 01/08/2020.

L. C. M. L. S. wrote the first draft of the manuscript and worked on it until its final shape as well as on the conducting of major interpretations. H. M. L. worked during field trips, sample collecting and helped with petrographic description and geochemical interpretations. G. A. L. worked on the main text and provided advisorship regarding the geology of the Alto Pajeú Terrane as well as on the granites of the Borborema Province. F. A. C. helped with the regional geology aspects, including bibliographic updating, text reviewing and geochronological data interpretation. J. F. A. N. worked on tables, text editing and conducted all steps of sample preparation for geochemistry. I. P. G. obtained the geochronological data and strongly contributed to the text and interpretation reviewing.

Competing interests: The authors have no competing interests to declare.

REFERENCES

Alcântara D.C.B.G., Uhlein A., Caxito F.A., Dussin I., Pedrosa-Soares A.C. 2017. Stratigraphy, tectonics and detrital zircon U-Pb (LA-ICP-MS) geochronology of the Rio Preto Belt and northern Paramirim corridor, NE, Brazil. *Brazilian Journal of Geology*, **47**(2):261-273. http://dx.doi.org/10.1590/2317-4889201720160102

Almeida F.F.M., Hasui Y., Brito Neves B.B., Fuck R.A. 1981. Brazilian structural provinces: an introduction. *Earth Science Reviews*, **17**(1-2):1-29. http://doi.org/10.1016/0012-8252(81)90003-9

Almeida F.F.M., Leonardos Jr. O.H. Valença J. 1967. Granitic rocks of Northeast South America. *In*: International Union of Geological Sciences. Recife: IUGS/UNESCO. 37 p.

Archanjo C.J., Hollanda M.H., Rodrigues S.O., Brito Neves B.B., Armstrong R. 2008. Fabrics of pre- and syntectonic granite plutons and chronology of shear zones in the Eastern Borborema Province, NE Brazil. *Journal of Structural Geology*, **30**(3):310-326. http://dx.doi.org/10.1016/j.jsg.2007.11.011

Barbarin B. 1999. A review of the relationships between granitoid types, their origins and their geodynamic environments. *Lithos*, **46**(3):605-626. http://dx.doi.org/10.1016/S0024-4937(98)00085-1

Basto C.F., Caxito F.A., Vale J.A.R., Silveira D.A., Rodrigues J.B., Alkmim A.R., Valeriano C.M., Santos E.J. 2019. An Ediacaran back-arc basin preserved in the Transversal Zone of the Borborema Province: evidence from geochemistry, geochronology and isotope systematics of the Ipueirinha Group, NE Brazil. *Precambrian Research*, **320**:213-231. https://doi.org/10.1016/j.precamres.2018.11.002

Bateman R. 1989. Cannibal Creek Granite: Post-tectonic "ballooning" pluton or pre-tectonic piercement diapir?: A Discussion. *The Journal of Geology*, **97**(6):766-768. http://dx.doi.org/10.1086/629360

Bonin B. 2007. A-type granites and related rocks: Evolution of a concept, problems and prospects. *Lithos*, **97**(1-2):1-29. https://doi.org/10.1016/j.lithos.2006.12.007

Brito Neves B.B. 1975. *Regionalização geotectônica do Pré-Cambriano nordestino*. PhD Thesis, Instituto de Geociências, Universidade de São Paulo, São Paulo, 198 p.

Brito Neves B.B., Fuck R.A., Pimentel M.M. 2014. The Brasiliano collage in South America: a review. *Brazilian Journal of Geology*, **44**(3):493-518. http://dx.doi.org/10.5327/Z2317-4889201400030010

Brito Neves B.B., Passarelli C.R., Basei M.A.S., Santos E.J. 2003. Idades U-Pb em zircão de alguns granitos clássicos da Província Borborema. *Geologia USP - Série Científica*, **3**:25-38. https://doi.org/10.5327/S1519-874X2003000100003

Brito Neves B.B., Santos E.J., Fuck R. A., Santos, L.C.M.L. 2016. A preserved early Ediacaran magmatic arc at the northernmost portion of the Transversal Zone central subprovince of the Borborema Province, Northeastern South America. *Brazilian Journal of Geology*, **46**(4):491-508. http://dx.doi.org/10.1590/2317-4889201620160004

Brito Neves B.B., Santos E.J., Van Schmus W.R. 2000. Tectonic History of the Borborema Province. *In*: Cordani U.G., Milani E.J., Tomaz Filho A., Campos D.A. (eds.), *Tectonic Evolution of South America*. 31st International Geological Congress. Rio de Janeiro, p. 151-182.

Castillo P.R. 2012. Adakite petrogenesis. *Lithos*, **134-135**:304-316. https://doi.org/10.1016/j.lithos.2011.09.013

Caxito F.A., Uhlein A., Dantas E.L. 2014a. The Afeição augen-gneiss Suite and the record of the Cariris Velhos Orogeny (1000-960 Ma) within the Riacho do Pontal fold belt, NE Brazil. *Journal of South American Earth Sciences*, **51**:12-27. https://doi.org/10.1016/j.jsames.2013.12.012

Caxito F.A., Uhlein A., Dantas E.L., Stevenson R., Salgado S.S., Dussin I.A., Sial A.N. 2016. A complete Wilson Cycle recorded within the Riacho do Pontal Orogen, NE Brazil: Implications for the Neoproterozoic evolution of the Borborema Province at the heart of *West Gondwana*. *Precambrian Research*, **282**:97-120. http://doi.org/10.1016/j.precamres.2016.07.001

Caxito F.A., Ulhein A., Stevenson R., Ulhein G. 2014b. Neoproterozoic oceanic crust remnants in northeast Brazil. *Geology*, **42**(5):387-390. https://doi.org/10.1130/G35479.1

Chappell B.W., White A.J.R. 1974. Two contrasting granite types. *Pacific Geology*, **8**:173-174.

Chappell B.W., White A.J.R. 2001. Two contrasting granite types: 25 years later. *Australian Journal of Earth Sciences*, **48**(4):489-499. https://doi.org/10.1046/j.1440-0952.2001.00882.x

Costa F.G., Klein E.L., Lafon J.M., Milhomem Neto J.M., Galarza M.M., Rodrigues J.B., Naleto J.L.C., Lima R.G.C. 2018. Geochemistry and U–Pb–Hf zircon data for plutonic rocks of the Troia Massif, Borborema Province, NE Brazil: Evidence for reworking of Archean and juvenile Paleoproterozoic crust during Rhyacian accretionary and collisional tectonics. *Precambrian Research*, **311**:167-194. https://doi.org/10.1016/j.precamres.2018.04.008

Cruden A.R. 1990. Flow and fabric development during the diapiric rise of magma. *The Journal of Geology*, **98**(5):681-698.

Cruden A.R., Weinberg R.F. 2018. Mechanisms of magma transport and storage in the lower and middle crust — magma segregation, ascent and emplacement. *Volcanic and Igneous Plumbing Systems*, 13-53. http://doi.org/10.1016/b978-0-12-809749-6.00002-9

Dantas E.L., Souza Z.S., Wernick E., Hackspacher P.C., Martin H., Xiadong D., Li J.W. 2013. Crustal growth in the 3.4-2.7 Ga São José do Campestre Massif, Borborema Province, NE Brazil. *Precambrian Research*, **227**:120-156. http://doi.org/10.1016/j.precamres.2012.08.006

De La Roche H., Leterrier J., Grandclaude P., Marchal M. 1980. A classification of volcanic and plutonic rocks using R_1R_2-diagram and major element analyses: its relationships with current nomenclature. *Chemical Geology*, **29**(1-4):183-210. https://doi.org/10.1016/0009-2541(80)90020-0

Defant M.J., Drummond M.S. 1990. Derivation of some modern arc magmas by melting of young subducted lithosphere. *Nature*, **347**:662-665. https://doi.org/10.1038/347662a0

Dhuime B., Hawkesworth C.J., Cawood P.A., Storey C.D. 2012. A change in the geodynamics of continental growth 3 billion years ago. *Science*, **335**(6074):1334-1336. https://doi.org/10.1126/science.1216066

Ferreira V.P., Sial A.N., Jardim de Sá E.F. 1998. Geochemical and isotopic signatures of Proterozoic granitoids in terranes of Borborema province, northeastern Brazil. *Journal of South America Earth Sciences*, **11**(5):439-455. https://doi.org/10.1016/S0895-9811(98)00027-3

Ferreira V.P., Valley J.W., Sial A.N., Spicuzza M. 2003. Oxygen isotope compositions and magmatic epidote from two contrasting metaluminous granitoids, NE Brazil. *Contributions to Mineralogy and Petrology*, **145**:205-216. https://doi.org/10.1007/s00410-003-0443-4

Fetter A.H., Santos T.J.S., Van Schmus W.R., Hackspacher P.C., Brito Neves B.B., Arthaud M.H., Nogueira Neto J.A., Wernick E. 2003. Evidence for Neoproterozoic continental arc magmatism in the Santa Quiteria Batholith of Ceará State, NW Borborema Province, NE Brazil: implications for the assembly of West Gondwana. *Gondwana Research*, **6**(2):265-273. https://doi.org/10.1016/S1342-937X(05)70975-8

Foley S.F., Barth M.G., Jenner G.A. 2000. Rutile/melt partition coefficient for trace elements and an assessment of the influence of rutile on the trace element characteristics of subduction zone magmas. *Geochimica et Cosmochimica Acta*, **64**(5):933-938. https://doi.org/10.1016/S0016-7037(99)00355-5

Frost B.R., Barnes C.G., Collins W.J., Arculus R.J., Ellis D.J., Frost C.D. 2001. A geochemical classification for granitic rocks. *Journal of Petrology*, **42**(11):2033-2048. https://doi.org/10.1093/petrology/42.11.2033

Ganade de Araújo C.E., Cordani U.G., Agbossoumounde Y., Caby R., Basei M.A.S., Weinberg R.F., Sato K. 2016. Tightening-up NE Brazil and NW Africa connections: New U–Pb/Lu–Hf zircon data of a complete plate tectonic cycle in the Dahomey belt of the West Gondwana Orogen in Togo and Benin. *Precambrian Research*, **276**:24-42. https://doi.org/10.1016/j.precamres.2016.01.032

Ganade de Araújo C.E., Cordani U.G., Weinberg R.F., Basei M.A.S., Armstrong R., Sato K. 2014a. Tracing Neoproterozoic subduction in the Borborema Province (NE-Brazil): Clues from U-Pb geochronology and Sr-Nd-Hf-O isotopes on granitoids and migmatites. *Lithos*, **202-203**:167-189. https://doi.org/10.1016/j.lithos.2014.05.015

Ganade de Araújo C.E., Rubatto D., Hermann J., Cordani U.G., Caby R., Basei M.A.S. 2014b. Ediacaran 2,500-km-long synchronous deep continental subduction in the West Gondwana Orogen. *Nature Communications*, **5**:5198. https://doi.org/10.1038/ncomms6198

Ganade de Araújo C.E., Weinberg R.F., Cordani U.G. 2014c. Extruding the Borborema Province (NE-Brazil): a two-stage Neoproterozoic collision process. *Terra Nova*, **26**(2):157-168. https://doi.org/10.1111/ter.12084

Gao Y., Hou Z., Kamber B.S., Wei R., Meng X., Zhao R. 2007. Adakite-like porphyries from the southern Tibetan continental collision zones: evidence for slab melt metasomatism. *Contributions to Mineralogy and Petrology*, **153**:105-120. https://doi.org/10.1007/s00410-006-0137-9

Gill J.B. 1981. *Orogenic andesites and plate tectonics*. Berlin: Springer.

Glazner A.F., Bartley J.M. 2006. Is stoping a volumetrically significant pluton emplacement process? *Geological Society of America Bulletin*, **118**(9-10):1185-1195. https://doi.org/10.1130/B25738.1

Guimarães I.P., Brito M.F.L., Lages G.A., Silva Filho A.F., Santos L., Brasilino R.G. 2016. Tonian granitic magmatism of the Borborema Province, NE Brazil: A review. *Journal of South American Earth Sciences*, **68**:97-112. https://doi.org/10.1016/j.jsames.2015.10.009

Guimarães I.P., Silva Filho A.F. 2000. Evidence of multiple sources involved in the genesis of the Neoproterozoic Itapetim granitic complex, NE Brazil, based on geochemical and isotopic data. *Journal of South American Earth Sciences*, **13**(6):561-586. https://doi.org/10.1016/S0895-9811(00)00040-7

Guimarães I.P., Silva Filho A.F., Almeida C.N., Macambira M.B., Armstrong R. 2011. U–Pb SHRIMP data constraints on calc-alkaline granitoids with 1.3–1.6 Ga Nd T_{DM} model ages from the central domain of the Borborema province, NE Brazil. *Journal of South American Earth Sciences*, **31**(4):383-396. https://doi.org/10.1016/j.jsames.2011.03.001

Guimarães I.P., Silva Filho A.F., Almeida C.N., Van Schmus W.R., Araújo J.M.M., Melo S.C., Melo E.B. 2004. Brasiliano (Pan-African) granite magmatism in the Pajeú-Paraíba belt, Northeast Brazil: an isotopic and geochronological approach. *Precambrian Research*, **135**(1-2):23-53. https://doi.org/10.1016/j.precamres.2004.07.004

Guimarães I.P., Silva Filho A.F., Melo S.C., Macambira M.B. 2005. Petrogenesis of A-type granitoids from the Pajeú-Paraíba Belt, Borborema Province, NE Brazil: constraints from geochemistry and isotopic composition. *Gondwana Research*, **8**(3):347-362. https://doi.org/10.1016/S1342-937X(05)71140-0

Guimarães I.P., Van Schmus W.R., Brito Neves B.B., Bittar S.M.B., Silva Filho A.F., Armstrong R. 2012. U–Pb zircon ages of orthogneisses and supracrustal rocks of the Cariris Velhos belt: Onset of Neoproterozoic rifting in the Borborema Province, NE Brazil. *Precambrian Research*, **192-195**:52-77. https://doi.org/10.1016/j.precamres.2011.10.008

Gutiérrez F., Payacán I., Szymanowski D., Guillong M., Bachmann O., Parada M.A. 2018. Lateral magma propagation during the emplacement of La Gloria Pluton, Central Chile. *Geology*, **46**(12):1051-1054. https://doi.org/10.1130/G45361.1

Hawkesworth C.J., Dhuime B., Pietranik A.B., Cawood P.A., Kemp A.I.S., Storey C.D. 2010. The generation and evolution of the continental crust. *Journal of the Geological Society*, **167**(2):229-248. http://dx.doi.org/10.1144/0016-76492009-072

Hutton D.H.W. 1988. Granite emplacement mechanisms and tectonic controls: inferences from deformation studies. *Transactions of the Royal Society of Edinburgh*, **79**(2-3):245-255. https://doi.org/10.1017/S0263593300014255

Janoušek V., Farrow C.M., Erban V. 2006. Interpretation of whole-rock geochemical data in igneous geochemistry: introducing Geochemical Data Toolkit (GCDkit). *Journal of Petrology*, **47**(6):1255-1259. https://doi.org/10.1093/petrology/egl013

Klemme S., Günther D., Hametner K., Prowatke S., Zack T. 2006. The partitioning of trace elements between ilmenite, ulvospinel, armalcolite and silicate melts with implications for the early differentiation of the moon. *Chemical Geology*, **234**(3-4):251-263. https://doi.org/10.1016/j.chemgeo.2006.05.005

Koepke J., Berndt J., Feig S.T., Holtz F. 2006. The formation of SiO_2-rich melts within the deep oceanic crust by hydrous partial melting of gabbros. *Contributions to Mineralogy and Petrology*, **153**:67-84. http://dx.doi.org/10.1007/s00410-006-0135-y

Kozuch M. 2003. *Isotopic and trace element geochemistry of Early Neoproterozoic gneissic and metavolcanic rocks in the Cariris Velhos orogen of the Borborema Province, Brazil, and their bearing on tectonic setting*. PhD Thesis, Department of Geology, University of Kansas, Lawrence, 199 p.

Kusumoto S., Takemura K. 2003. Numerical simulation of caldera formation due to collapse of a magma chamber. *Geophysical Research Letters*, **30**(24):2278. http://dx.doi.org/10.1029/2003GL018380

Lages G.A., Dantas E.L. 2016. Floresta and Bodocó mafic-ultramafic complexes, western Borborema Province, Brazil: geochemical and isotope constraints for evolution of a Neoproterozoic arc environment and retro-eclogitic hosted Ti-mineralization. *Precambrian Research*, **280**:95-119. https://doi.org/10.1016/j.precamres.2016.04.017

Lages G.A., Marinho M.S., Nascimento M.A.L., Medeiros V.C., Dantas E.L. 2016. Geocronologia e aspectos estruturais e petrológicos do Pluton Bravo, Domínio Central da Província Borborema, Nordeste do Brasil: um granito transalcalino precoce no estágio pós-colisional da Orogênese Brasiliana. *Brazilian Hournal of Geology*, **46**:41-61.

Lages G.A., Santos L.C.M.L., Brasilino R.G., Rodrigues J.B., Dantas E.L. 2019. Statherian-Calymmian (ca. 1.6 Ga) magmatism in the Alto Moxotó Terrane, Borborema Province, northeast Brazil: Implications for within-plate and coeval collisional tectonics in West Gondwana. *Journal of South American Earth Sciences*, **91**:116-130. https://doi.org/10.1016/j.jsames.2019.02.003

Lameyre J., Bowden P. 1982. Plutonic rock type series: discrimination of various granitoid series and related rocks. *Journal of Volcanology and Geothermal Research*, **14**(1-2):169-186. https://doi.org/10.1016/0377-0273(82)90047-6

Lima M.I.C., Gava A., Fernandes P.E.C.A., Pires J.L., Siga Jr. O. 1985. *Projeto ferro titanado de Floresta*. Minérios de Pernambuco/Radambrasil. v. 1. 314 p.

Lima J.V., Guimarães I.P., Santos L., Amorim J.V.A., Farias D.J.S. 2017. Geochemical and isotopic characterization of the granitic magmatism along the Remígio - Pocinhos shear zone, Borborema Province, NE Brazil. *Journal of South American Earth Sciences*, **75**:116-133. https://doi.org/10.1016/j.jsames.2017.02.004

Lima H.M., Pimentel M.M., Fuck R.A., Santos L.C.M.L., Dantas E.L. 2018. Geochemical and detrital zircon geochronological investigation of the metavolcanosedimentary Araticum complex, sergipano fold belt: Implications for the evolution of the Borborema Province, NE Brazil. *Journal of South American Earth Sciences*, **86**:176-192. https://doi.org/10.1016/j.jsames.2018.06.013

Lima H.M., Pimentel M.M., Santos L.C.M.L., Dantas E.L. 2019. Isotopic and geochemical characterization of the metavolcano-sedimentary rocks of the Jirau do Ponciano dome: A structural window to a Paleoproterozoic continental arc root within the Southern Borborema Province, Northeast Brazil. *Journal of South American Earth Sciences*, **90**:54-69. https://doi.org/10.1016/j.jsames.2018.12.002

Ludwig K.R. 2012. *User's Manual for Isoplot Version 3.75-4.15:* A Geochronological Toolkit for Microsoft Excel. Berkeley Geochronological Center Special Publication, 5.

Magee C., Muirhead J.D., Karvelas A., Holford S.P., Jackson C.A.L., Bastow I.D., Schofield N., Stevenson C.T.E., McLean C., McCarthy W., Shtukert O. 2016. Lateral magma flow in mafic sill complexes. *Geosphere*, **12**(3):809-841. https://doi.org/10.1130/GES01256.1

Maniar P.D., Piccoli P.M. 1989. Tectonic discrimination of granitoids. *Geological Society of America Bulletim*, **101**(5):635-643. https://doi.org/10.1130/0016-7606(1989)101<0635:TDOG>2.3.CO;2

Martin H., Smithies R.H., Rapp R., Moyen J.F., Champion D. 2005. An overview of adakite, TTG and sanukitoid: relationships and some implications for crustal evolution. *Lithos*, **79**(1-2):1-24. https://doi.org/10.1016/j.lithos.2004.04.048

McMillan N.J., Harmon R.S., Moorbath S., Lopez-Escobar L., Strong D.F. 1989. Crustal sources involved in continental arc magmatism: A case study of volcan Mocho-Choshuenco, southern Chile. *Geology*, **17**(12):1152-1156. https://doi.org/10.1130/0091-7613(1989)017<1152:CSIICA>2.3.CO;2

Medeiros V.C. 2004. *Evolução geodinâmica e condicionamento estrutural dos terrenos PiancóAlto Brígida e Alto Pajeú, domínio da zona transversal NE do Brasil*. PhD Thesis. Centro de Ciências Exatas e da Terra, Universidade Federal do Rio Grande do Norte, Natal, 200 p.

Nakamura N. 1974. Determination of REE, Ba, Fe, Mg, Na and K in carbonaceous and ordinary chondrites. *Geochimica et Cosmochimica Acta*, **38**(5):757-775. https://doi.org/10.1016/0016-7037(74)90149-5

Nascimento M.A.L. Galindo A.C. Medeiros V.C. 2015. Ediacaran to Cambrian magmatic suites in the Rio Grande do Norte domain, extreme Northeastern Borborema Province (NE of Brazil): Current knowledge. *Journal of South American Earth Sciences*, **58**:281-299. https://doi.org/10.1016/j.jsames.2014.09.008

Neal C.R., Taylor L.A. 1989. A negative Ce anomaly in a peridotite xenolith: Evidence for crustal recycling into the mantle or mantle metasomatism? *Geochimica et Cosmochimoca Acta*, **53**(5):1035-1040. https://doi.org/10.1016/0016-7037(89)90208-1

Neves S.P. 2015. Constraints from zircon geochronology on the tectonic evolution of the Borborema Province (NE Brazil): Widespread intracontinental Neoproterozoic reworking of a Paleoproterozoic accretionary orogen. *Journal of South American Earth Sciences*, **58**:150-164. http://dx.doi.org/10.1016/j.jsames.2014.08.004

Neves S.P., Bruguier O., Vauchez A., Bosch D., Silva J.M.R., Mariano G. 2006. Timing of crust formation, deposition of supracrustal sequences, and Transamazonian and Brasiliano metamorphism in the East Pernambuco belt (Borborema Province, NE Brazil): implications for western Gondwana assembly. *Precambrian Research*, **149**(3-4):197-216. https://doi.org/10.1016/j.precamres.2006.06.005

Oliveira E.P., Windley B.F. Araújo M.N.C. 2010. The Neoproterozoic Sergipano orogenic belt, NE Brazil: A complete plate tectonic cycle in western Gondwana. *Precambrian Research*, **181**(1-4):64-84. http://doi.org/10.1016/j.precamres.2010.05.014

Oliveira R.G., Medeiros W.E. 2018. Deep crustal framework of the Borborema Province, NE Brazil, derived from gravity and magnetic data. *Precambrian Research*, **315**:45-65. https://doi.org/10.1016/j.precamres.2018.07.004

Paces J.B., Miller Jr. J.D. 1993. Precise U-Pb ages of Duluth Complex and related mafic intrusions, northeastern Minnesota: geochronological insights to physical, petrogenetic, paleomagnetic and tectonomagmatic processes associated with the 1.1 Ga midcontinent rift system. *Journal of Geophysical Research*, **98**(B8):13997-14013. https://doi.org/10.1029/93JB01159

Paterson S.R., Fowler Jr. T.K. 1993. Re-examining pluton emplacement processes. *Journal of Structural Geology*, **15**(2):191-206. https://doi.org/10.1016/0191-8141(93)90095-R

Pearce J.A., Harris N.B.W., Tindle A.G. 1984. Trace element discrimination diagrams for the tectonic interpretation of granitic rocks. *Journal of Petrology*, **25**(4):956-983. https://doi.org/10.1093/petrology/25.4.956

Petford N., Cruden A.R., McCaffrey K.J.W., Vigneresse J.-L. 2000. Granite magma formation, transport and emplacement in the Earth's crust. *Nature*, **408**:669-673. https://doi.org/10.1038/35047000

Rapp R.P., Shimizu N., Norman M.D., Applegate G.S. 1999. Reaction between slab-derived melts and peridotite in the mantle wedge: experimental constraints at 3.8 GPa. *Chemical Geology*, **160**(4):335-356. https://doi.org/10.1016/S0009-2541(99)00106-0

Rapp R.P., Xiao L., Shimuzu N. 2002. Experimental constraints on the origin of potassium-rich adakite in east China. *Acta Petrologica Sinica*, **18**(3):293-302.

Rapp R.P., Watson E.B. 1995. Dehydration melting of metabasalt at 8–32 kbar, implications for continental growth and crust–mantle recycling. *Journal of Petrology*, **36**(4):891-931. https://doi.org/10.1093/petrology/36.4.891

Rochira F., Caggianelli A., de Lorenzo S. 2018. Regional thermo-rheological field related to granite emplacement in the upper crust: implications for the Larderello area (Tuscany, Italy), *Geodinamica Acta*, **30**(1):225-240. https://doi.org/10.1080/09853111.2018.1488912

Rollinson H. 2009. New models for the genesis of plagiogranites in the Oman ophiolite. *Lithos*, **112**(3-4):603-614. https://doi.org/10.1016/j.lithos.2009.06.006

Sajona F.G., Maury R.C., Bellon H., Cotten J., Defant M. 1996. High field strength element enrichment of Pliocene–Pleistocene island arc basalts, Zamboanga Peninsula, Western Mindanao (Philippines). *Journal of Petrology*, **37**(3):693-726. https://doi.org/10.1093/petrology/37.3.693

Sajona F.G., Maury R.C., Pubellier M., Leterrier J., Bellon H., Cotten J. 2000. Magmatic source enrichment by slab-derived melts in a young post-collision setting, central Mindanao (Philippines). *Lithos*, **54**(3-4):173-206. https://doi.org/10.1016/S0024-4937(00)00019-0

Santos E.J. 1995. *O complexo granítico Lagoa das Pedras: acreção e colisão na região de Floresta (Pernambuco), Província Borborema*. PhD Thesis, Instituto de Geociências, Universidade de São Paulo, São Paulo, 228 p.

Santos E.J., Medeiros V.C. 1999. Constraints from granitic plutonism on Proterozoic crustal growth of the Transverse Zone, Borborema Province, NE-Brazil. *Revista Brasileira de Geociências*, **29**(1):73-84. https://doi.org/10.25249/0375-7536.1999297384

Santos E.J., Van Schmus W.R., Kozuch M., Brito Neves B.B. 2010. The Cariris Velhos tectonic event in northeast Brazil. *Journal of South American Earth Sciences*, **29**(1):61-76. https://doi.org/10.1016/j.jsames.2009.07.003

Santos L.C.M.L., Dantas E.L., Cawood P.A., Lages G.A., Lima H.M., Santos E.J. 2018. Accretion tectonics in Western Gondwana deduced from Sm-Nd Isotope mapping of terranes in the Borborema Province, NE Brazil. *Tectonics*, **37**(8):2727-2743. https://doi.org/10.1029/2018TC005130

Santos L.C.M.L., Dantas E.L., Cawood P.A., Lages G.A., Lima H.M., Santos E.J., Caxito F.A. 2019. Early to late Neoproterozoic subduction-accretion episodes in the Cariris Velhos Belt of the Borborema Province, Brazil: Insights from isotope and whole-rock geochemical data of supracrustal and granitic rocks. *Journal of South American Earth Sciences*, **96**:1-22. https://doi.org/10.1016/j.jsames.2019.102384

Santos L.C.M.L., Dantas E.L., Cawood P.A., Santos E.J., Fuck R.A. 2017a. Neoarchean crustal growth and Paleoproterozoic reworking in the Borborema Province, NE Brazil: insights from geochemical and isotopic data of TTG and metagranitic rocks of the Alto Moxotó Terrane. *Journal of South American Earth Sciences*, **79**:342-363. http://doi.org/10.1016/j.jsames.2017.08.013

Santos L.C.M.L., Dantas E.L., Santos E.J., Santos R.V., Lima H.M. 2015. Early to late Paleoproterozoic magmatism in NE Brazil: The Alto Moxotó Terrane and its tectonic implications for the pre-West Gondwana assembly. *Journal of South American Earth Sciences*, **58**:188-209. http://doi.org/10.1016/j.jsames.2014.07.006

Santos L.C.M.L., Dantas E.L., Vidotti R.M., Cawood P.A., Santos E.J., Fuck R.A., Lima H.M. 2017b. Two-stage terrane assembly in Western Gondwana: Insights from structural geology and geophysical data of central Borborema Province, NE Brazil. *Journal of Structural Geology*, **103**:167-184. http://doi.org/10.1016/j.jsg.2017.09.012

Santos L.C.M.L., Fuck R.A., Santos E.J., Dantas E.L. 2014. Análise tectônica de terrenos: metodologia, aplicação em cinturões orogênicos e exemplos das províncias Tocantins e Borborema, Brasil. *Geonomos*, **22**(2):51-63. https://doi.org/10.18285/geonomos.v22i2.317

Santos T.J.S., Fetter A.H., Hackspacher P.C., Schmus W.R.V., Nogueira Neto J.A. 2008. Neoproterozoic tectonic and magmatic episodes in the NW sector of the Borborema Province, NE Brazil, during assembly of western Gondwana. *Journal of South American Earth Sciences*, **25**(3):271-284. http://dx.doi.org/10.1016/j.jsames.2007.05.006

Sen C., Dunn T. 1994. Dehydration melting of a basaltic composition amphibolite at 1.5 GPa and 2.0 GPa: implication for the origin of adakites. *Contributions to Mineralogy and Petrology*, **117**:394-409. https://doi.org/10.1007/BF00307273

Sheth H.C., Torres-Alvarado I.S., Verma S.P. 2002. What Is the "Calc-alkaline Rock Series"? *International Geology Review*, **44**(8):686-701. https://doi.org/10.2747/0020-6814.44.8.686

Sial A.N. 1987. Granitic rocks of Northeast Brazil. *In*: International Symposium on Granites and Associated Mineralizations, 1., Salvador. *Extended Abstracts*. Salvador: SGM. p. 61-69.

Sial A.N. 1990. Epidote-bearing calc-alkaline granitoids in Northeast Brazil. *Revista Brasileira de Geociências*, **20**(1-4):88-100.

Sial A.N., Ferreira V.P. 2016. Magma association in Ediacaran granitoids of the Cachoeirinha-Salgueiro and Alto Pajeú terranes, northeastern Brazil: Forty years of studies. *Journal of South American Earth Sciences*, **68**:113-133. https://doi.org/10.1016/j.jsames.2015.10.005

Silva Filho A.F., Guimarães I.P., Ferreira V.P., Armstrong R., Sial A.N. 2010. Ediacaran Águas Belas pluton, Northeastern Brazil: Evidence on age, emplacement and magma sources during Gondwana amalgamation. *Gondwana Research*, **17**(4):676-687. https://doi.org/10.1016/j.gr.2009.10.002

Sisson T.W., Grove T.L. 1993. Experimental investigations of the role of H_2O in calc-alkaline differentiation and subduction zone magmatism. *Contributions to Mineralogy and Petrology*, **113**:143-166. https://doi.org/10.1007/BF00283225

Skjerlie K.P., Patiño Douce A.E. 2002. The fluid-absent partial melting of a zoisite-bearing quartz eclogite from 1.0 to 3.2 Gpa: implications for melting in thickened continental crust and for subduction-zone processes. *Journal of Petrology*, **43**(2):291-314. https://doi.org/10.1093/petrology/43.2.291

Stern R.A. 1997. The GSC Sensitive High-Resolution Ion Microprobe (SHRIMP): analytical techniques of zircon U-Th-Pb age determinations and performance evaluation. *In*: Radiogenic age and isotopic studies: Report 10; Geological Survey of Canada, Current Research 1997-F, p. 1-31. https://doi.org/10.4095/209089

Streckeisen A. 1976. To each plutonic rock its proper name. *Earth-Science Reviews*, **12**(1):1-33. https://doi.org/10.1016/0012-8252(76)90052-0

Sun S.S., McDonough W.F. 1989. Chemical and isotopic systematics of oceanic basalts: implications for the mantle composition and processes. *In*: Saunders A.D., Norry M.J. (Eds.). *Magmatism in the ocean basins*. London, Geological Society of London Special Publication, **42**:313-345. https://doi.org/10.1144/GSL.SP.1989.042.01.19

Tang G., Wang Q., Wyman D.A., Li Z.-X., Zhao Z.-H., Jia X.-H., Jiang Z.-Q. 2010. Ridge subduction and crustal growth in the Central Asian Orogenic Belt: Evidence from Late Carboniferous adakites and high-Mg diorites in the western Junggar region, northern Xinjiang (west China). *Chemical Geology*, **277**(3-4):281-300. https://doi.org/10.1016/j.chemgeo.2010.08.012

Tapponnier P., Peltzer G., Le Dain A.Y., Armijo R., Cobbold P. 1982. Propagating extrusion tectonics in Asia: New insights from simple experiments with plasticine. *Geology*, **10**(12):611-616. https://doi.org/10.1130/0091-7613(1982)10<611:PETIAN>2.0.CO;2

Tikoff B., Teyssier C. 1994. Strain modeling of displacement-field partitioning in transpressional orogens. *Journal of Structural Geology*, **16**(11):1575-1588. https://doi.org/10.1016/0191-8141(94)90034-5

Trompette R. 1994. *Geology of Western Gondwana (2000-500 Ma): pan-African-Brasiliano aggregation of South America and Africa*. Rotterdam, Balkema, 350 p.

Van Schmus W.R., Brito Neves B.B., Hackspacher P., Babinski M. 1995. U/Pb and Sm/Nd geochronologic studies of eastern Borborema Province, northeastern Brazil: initial conclusions. *Journal of South American Earth Sciences*,**8**(3-4):267-288.https://doi.org/10.1016/0895-9811(95)00013-6

Van Schmus W.R., Brito Neves B.B., Williams I.S, Hackspacher P.C., Fetter A.H., Dantas E.L., Babinski M. 2003. The Seridó Group of NE Brazil, a late Neoproterozoic pre- to syn-collisional basin in West Gondwana: insights from SHRIMP U–Pb detrital zircon ages and Sm–Nd crustal residence (T_{DM}) ages. *Precambrian Research*, **127**(4):287-327. https://doi.org/10.1016/S0301-9268(03)00197-9

Van Schmus W.R., Kozuch M., Brito Neves B.B. 2011. Precambrian history of the Zona Transversal of the Borborema Province, NE Brazil: Insights from Sm-Nd and U-Pb geochronology. *Journal of South America Earth Sciences*, **31**(2-3):227-252. https://doi.org/10.1016/j.jsames.2011.02.010

Van Schmus W.R., Oliveira E.P., Silva Filho A.F., Toteu S.F., Penaye J., Guimarães I.P. 2008. Proterozoic links between the Borborema Province, NE Brazil, and the Central African Fold Belt. Geological Society, London, *Special Publications*, **294**:69-99. https://doi.org/10.1144/sp294.5

Vauchez A., Neves S.P., Caby R., Corsini M., Edydio-Silva M., Arthaud M., Amaro V.E. 1995. The Borborema shear zone system, NE Brazil. *Journal of South American Earth Sciences*, **8**(3-4):247-266. https://doi.org/10.1016/0895-9811(95)00012-5

Viegas L.G.F., Archanjo C., Vauchez A. 2013. Fabrics of migmatites and the relationships between partial melting and deformation in high-grade transpressional shear zones: the Espinho Branco anatexite (Borborema Province, NE Brazil). *Journal of Structural Geology*, **48**:45-56. https://doi.org/10.1016/j.jsg.2012.12.008

Viegas L.G.F., Archanjo C.J., Hollanda M.H.B.M., Vauchez A. 2014. Microfabrics and zircon U–Pb (SHRIMP) chronology of mylonites from the Patos shear zone (Borborema Province, NE Brazil). *Precambrian Research*, **243**:1-17. http://dx.doi.org/10.1016/j.precamres.2013.12.020

Wang Q., Xu J.-F., Jian P., Bao Z.-W., Zhao Z.-H., Li C.-F., Xiong X.-L., Ma J.-L. 2006. Petrogenesis of Adakitic Porphyries in an Extensional Tectonic Setting, Dexing, South China: Implications for the Genesis of Porphyry Copper Mineralization. *Journal of Petrology*, **47**(1):119-144. https://doi.org/10.1093/petrology/egi070

Weinberg R.F., Sial A.N., Mariano G. 2004. Close spatial relationship between plutons and shear zones. *Geology*, **32**(5):377-380. https://doi.org/10.1130/G20290.1

Williams I.S. 1998. U-Th-Pb geochronology by ion micro-probe. *In*: McKibben M.A., Shanks III W.C., Ridley W.I. (Eds.), *Applications of Microanalytical Techniques to Understanding Mineralization Processes.* Reviews in Economic Geology 7, El Paso, Texas, p. 1-75.

Yuguchi T., Nishiyama T. 2008. The mechanism of myrmekite formation deduced from steady-diffusion modeling based on petrography: Case study of the Okueyama granitic body, Kyushu, Japan. *Lithos*, **106**(3-4):237-260. https://doi.org/10.1016/j.lithos.2008.07.017

Žák J., Paterson S.R. 2006. Roof and walls of the Red Mountain Creek pluton, eastern Sierra Nevada, California (USA): implications for process zones during pluton emplacement. *Journal of Structural Geology*, **28**(4):575-587. https://doi.org/10.1016/j.jsg.2005.12.017